Study of Porous Lesions of the Anterior Femoral Neck (Cribra Femora) through Portable X-ray Fluorescence Spectrometry

Jacobs, Martijn

Study of Porous Lesions of the Anterior Femoral Neck (Cribra Femora) through Portable X-ray Fluorescence Spectrometry

Martijn Jacobs

Universiteit Leiden
The Netherlands

Study of Porous Lesions of the Anterior Femoral Neck (Cribra Femora) through Portable X-ray Fluorescence Spectrometry

Martijn Jacobs
S3384462

Master Thesis Archaeological Science
1084VTSY

Supervisors
Prof. Dr. Sarah Schrader
Prof. Dr. Dennis Braekmans

Leiden University, Faculty of Archaeology

Final Version

Acknowledgments

I would like to thank professor Sarah Schrader for allowing me to work on the Arnhem and Middenbeemster osteological for this master's thesis. Doing research on human remains has been a dream of mine since I first excavated skeletons in 2017. The same gratitude goes out to professor Dennis Braekmans for allowing me to use the brand new pXRF-machine, as well as Dr. Erik Mulder for showing me how to set it up and use it. I want to thank both my supervisors for all their corrections, ideas and suggestions.

I also would like to thank my parents and partner Vanshika, for supporting my plan to move to the Netherlands to study archaeological sciences. It was a great opportunity to be able to do this research and I must say that I learned a lot in the past year.

Martijn Jacobs

30/06/2023

Table of contents

List of Figures

List of Tables

1: Introduction

This master thesis focusses on cribra femora, which is a porous patch on the anterior neck of the femur. It is considered part of a larger family of such lesions called cribrous or porous lesions. The other members of this family are cribra orbitalia (porosity of the eye orbits), cribra cranii, also known as porotic hyperostosis (porosity of the cranial vault) and cribra humeri (porosity of the proximal humerus).

These porous lesions, in particular cribra orbitalia and cribra cranii, have been of interest in the field of archaeology, as they have been thought to result from iron deficiency anaemia and were therefore used as a proxy to study iron deficiency in ancient populations.

However, there is still no consensus on what causes these lesions to form. Traditionally, iron deficiency was considered to be the aetiology, whereby the human body would expand its red blood cell producing bone marrow in to make up for its lack in iron. This marrow expansion would put pressure on the thin cortical bone, resulting in these lesions.

Yet other researchers have proposed different types of anaemia or other nutritional deficiencies to be the underlaying cause. Some recent studies have even questioned whether they are the result of a pathology at all and in fact may be simple anatomical variation.

Figure 1: Cribra Femora. Examples of cribra femora on the anterior femoral necks of a juvenile (left) and adult (right) from Middenbeemster. (Photograph by Martijn Jacobs)

Figure 2: Cribra orbitalia. Example of cribra orbitalia in an adolescent from Arnhem. (Photograph by Martijn Jacobs).

In this study, we will focus on the specific type of porous lesion that can be found on the neck of the femur, cribra femora. Although it is very common, especially in sub-adults, very little research has focussed on this type of porous lesion.

Thus far, most research on this subject has refrained from looking at bone chemistry, often using purely macroscopic evaluation of the lesions. Therefore, in this thesis we would like to introduce the technique of portable X-ray Fluorescence Spectrometry (pXRF) to look at the elemental composition of human bones.

pXRF uses X-rays to excite the electrons of atoms in a sample, which causes fluorescent photons to be emitted by the elements in the samples. Measuring these photons, pXRF can identify and quantify the individual elements that make up the sample. It is also completely harmless towards the sample under study.

In this thesis, the main research question is whether iron deficiency anaemia is the main cause of cribra femora? We will identify cribra femora and cribra orbitalia on a selection of skeletons from the archaeological sites of Middenbeemster and Arnhem. For each skeleton, we will then measure the elemental concentrations in its bones. The elemental concentrations of skeletons with and without cribra femora will then be compared with each other through statistical tests.

It is our hypothesis that if cribra femora is indeed caused by acute iron deficiency, skeletons with cribra femora will have iron concentrations that are statically significantly lower than those without cribra femora. If there is no significant difference in iron concentrations between both groups, iron deficiency anaemia can not be considered to be the aetiology of cribra femora.

Secondly, the archaeological sites of Middenbeemster and Arnhem differ in geographical location and socio-economic state of the deceased. Associated differences in diet will possibly also cause differences in elemental concentrations of bone. Therefore a secondary hypothesis is formed, which says that most elemental concentrations at Middenbeemster will differ significantly from those at Arnhem, allowing to distinguish between the two archaeological sites.

Lay-out of thesis

The following chapters will consist of a background chapter, materials chapter, methods chapter, results chapter, discussion chapter and finally the conclusion chapter. The background chapter will have three subsections, the first of which is a discussion on porous lesions (their occurrence, frequencies, and aetiology. The second subsection of the background chapter is a discussion on the workings of pXRF and an evaluation of the different pXRF set-up's by previous researchers. The final subsection concerns the archaeological contexts of the Middenbeemster and Arnhem sites.

The materials chapter will go into detail on the selection of the skeletons from the Arnhem and Middenbeemster osteological collections. In the materials chapter, the pXRF set-up developed for this thesis will be explained. The results are then discussed in the discussion chapter before final conclusions are drawn.

2: Background

This chapter will provide more detailed information on the different aspects of this master thesis. First, cribra femora and cribra orbitalia will be defined more in depth, followed by a discussion of the status quaestionis of research regarding their frequency, location and aetiology.

This is followed by a detailed explanation of the concepts behind portable X-ray fluorescence spectrometry and its current applications in archaeology and osteoarchaeology. Finally, this background chapter will discuss the archaeological contexts of the sites at Middenbeemster and Arnhem.

2.1 Cribra Femora

In this study, we define cribra femora as present when there is a patch of fine porosity present on the anterior or medio-anterior surface of the femoral neck (see Figure 1 & 2). The size of this lesion can vary from less than a centimetre up to several centimetres in cross-section. It is usually found bilaterally. In juvenile bones the porosity often extends more to the lateral section of the femoral neck. When diagnosing cribra femora, it is important to make sure that the surface of the porous lesion is at the same height as the non-porous cortical bone surrounding it. In cases where a section of cortical bone from the femoral neck is absent, thereby exposing the underlaying trabecular bone in a depression that can measure several centimetres in cross-section, this should not be diagnosed as cribra femora but instead as Allen's fossa, also known as the cervical fossa of Allen (Göhring, 2020). This is a bilateral non-metric trait and therefore does not implicate any pathology (see Figure 3). It can be most easily recognized by the presence of distinct cortical bone margins. (Göhring, 2020; Vyas et al., 2013).

Figure 3: Allen's Fossa. Example of Allan's Fossa on an adult femur from Arnhem. (Photograph by Martijn Jacobs).

2.2 Cribra Orbitalia

For cribra orbitalia, we use the definition of Zdilla et al. (2021) who define it as a "morphological feature characterized by discontinuity in the smooth surface of the orbital roof" (p. 1628). It is most common

bilateral but can also appear unilateral (see Figure 3). There are many different scoring systems for severity, but in this paper only the presence or absence will be marked.

Of the four types of cribrous lesions, cribra orbitalia has received by far the highest amount of research attention, followed by porotic hyperostosis. The main reason for this increased attention results from the use of cribra orbitalia and porotic hyperostosis as stress markers. However, as will become clear in the aetiology section, there is still an active debate on the causes of these two pathologies.

2.3 Frequency of porous lesions

Both post-cranial porous lesions, cribra femora and cribra humeri, have been studied far less often than criba orbitalia and porotic hyperostosis, yet they are quite common, especially in sub-adults. In a large study covering multiple medieval and early modern sites from the Netherlands (N = 232), Schats (2021) found cribra femora to be present in 90.5% of children aged 4 – 12 and 80.8% of adolescents aged 13 – 19. Frequency goes down with age resulting in 38.5% in younger adults (aged 20 – 35) and finally 13.0% in older adults (aged 35+). Cribra femora is the most common of cribrous lesions followed by cribra orbitalia (52.4% in children, 20.5% in younger adults) and cribra humeri (38.1% in children, 15.4% in younger adults). All three show a peak frequency in childhood after which they go down (Schats 2021, pp. 84-85). In regards to the co-occurrence of the different lesions, each of them is still most likely to be found on its own, however a statistically significant correlation was found between cribra femora and cribra humeri (Schats 2021, p. 87).

Gomes et al (2022) did a similar study on sub-adults from Portugal, with the exception of one individual that was born in Africa. All individuals died between 1904 and 1932. The main differences with Schats (2021) are the smaller sample size (N = 56), the inclusion of cribra cranii (porotic hyperostosis) and the sample consisting completely out of sub-adults aged 7 to 19. Again cribra femora was found to be the most frequent with 69.6%, followed by cribra orbitalia at 47.3%, then cribra humeri with 26.8% and finally porotic hyperostosis at 10.9% (Gomes et al., 2022, p. 1063-1065). Cribra femora was shown to be significantly related to age-at-death, becoming less frequent as age increases.

2.4 Location of porous lesions

The location of porous lesions on the skeleton is dictated by the distribution and rate of conversion of the red bone marrow. Infants are born with solely red marrow, which starts to convert into fatty yellow marrow as the individual grows older. By the time they reach the age of 25, the appendicular skeleton has been almost completely converted to yellow marrow, with the exception of the proximal ends of the femora and humeri (see Figure 4). At this age, most of the red or mixed marrow is located in the cranium, vertebra, ribs, sternum and pelvis (Kricun, 1985, p. 12; Brickley, 2018). In the skull, marrow reconversion starts at the mandible and spreads in two ways posteriorly, meaning that the cranial vault is the last section of the skull to be converted. Brickley (2018) explains that porous lesions due to marrow hyperplasia can only appear in places where red or mixed marrow is present, because it is the marrow expansion that causes the atrophy of the cortical bone.

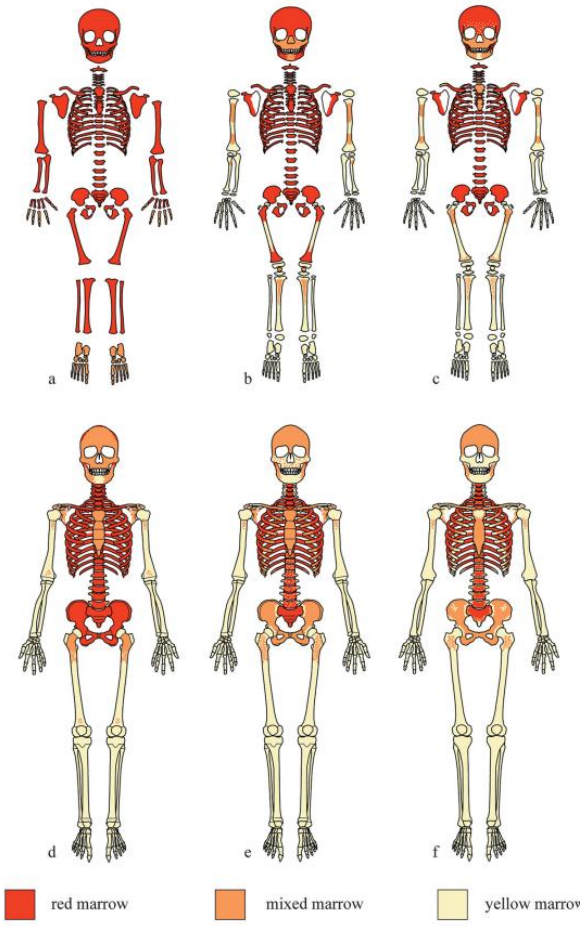

Figure 4: Bone conversion. Conversion of red bone marrow into yellow and mixed between infancy and the age of 25. (Brickley, 2018, p. 898).

It is however possible that some yellow marrow is reconverted into red marrow if the body needs to suddenly increase its production of red blood cells (Brickley, 2018, p. 899). For example, Kricun (1985) found reconverted red marrow in the distal right femur and throughout both tibia in a 31-year old patient who suffered from sickle cell anaemia (p. 17). The conversion process itself does not necessarily have to lead to marrow expansion. Besides anaemia, there are also other factors that can contribute to the reconversion of marrow such as smoking, obesity or diabetes (Malkiewicz & Dziedzig, 2012).

Given that infants and young children have almost exclusively red marrow, they would be much more vulnerable towards developing porous lesions when for any reason red blood cell production needs to be increased. They simply do not have the space to handle an increased red marrow volume and thus will easily build pressure, resulting in its cortical atrophy (Brickley, 2018).

2.5 Aetiology

Although porous lesions are very common, as of yet there has not been consensus on their aetiology. In this subsection, we will look at the traditional interpretations of porous lesions and the long discussion of their aetiology.

2.5.1 Anaemia

Traditionally, the occurrence of both cribra orbitalia and porotic hyperostosis has been connected with anaemia (Angel, 1966). This condition refers either to inadequate levels of haemoglobin in a patient's blood, which is the protein that binds oxygen in red blood cells, or a shortage of red blood cells themselves. There are various distinct types of anaemia such as iron deficiency anaemia, megaloblastic anaemia, sickle cell anaemia and thalassemia, which each cause insufficient haemoglobin levels or red blood cell counts through different mechanisms (Penn Medicine, 2023).

In cases of anaemia, hyperplasia of the hematopoietic (red) bone marrow could take place to increase red blood cell production. Brickley (2018) explains that the expanded marrow causes pressure that destroys the fine trabeculae and widens the remaining trabeculae through perforation an resorption. Eventually, this pressure can lead to the atrophy of the cortical bone. Less marrow expansion is needed for the orbital roof to be perforated, as it is much thinner than the cortical bone on the ectocranial surface of the cranial vault (p. 899).

In the mid 1960s, Angel (1966) connected both cribra orbitalia and porotic hyperostosis with hereditary hemolytic anaemias, more specifically with thalassemia and sickle cell anaemia. Hemolytic aneamias are caused by higher rates of hemolysis (red blood cell destruction) compared to erythropoiesis (red blood cell creation). In thalassemia, these discrepancies are caused by defects in the synthesis of one or more haemoglobin chains (Muncie & Campbell, 2009). Sickle cell anaemia is caused by mutations affecting the β-globin chain of haemoglobin creating sickle haemoglobin. Under specific conditions, this variant of normal haemoglobin can lead to the deformation of red blood cells into a distinct sickle shape (Chakravorty & Williams, 2015; Brandow & Liem, 2022). Both conditions are hereditary and offer some protection against falciparum malaria, which explains why they are found more frequently in populations from areas where malaria is common (Wambua et al., 2006; Serjeant, 2010).

However, due to the high frequency of porotic hyperostosis and cribra orbitalia, later researchers doubted that hereditary anaemias such as thalassemia and sickle cell anaemia were responsible for this. Carlson et al. (1974) in their study on Nubian skeletal remains, considers iron-deficiency anaemia a more plausible explanation for the high rate of cribra orbitalia in their sample, possibly worsened by internal bleeding caused by parasitic infection. They do nuance that it is possible for thalassemia and/or sickle cell anaemia to have been present in their population, but not to the extent of the attested frequency of cribra orbitalia. The mostly wheat-based diet of the Nubian population, as well as the habit of extended weaning of their children, would explain the high rate of iron-deficiency (Carlson et al, 1974).

In the 1980s, Stuart-Macadam (1985) challenges the idea that porotic hyperostosis represents an episode of anaemia during or shortly before death. Based on skeletons from Poundbury Camp, she demonstrates that porotic hyperostosis most likely forms during childhood and that its presence among older individuals is the result from a childhood episode that has not fully remodelled. A study by Obertova & Thurzo (2004) on an early medieval collection from Slovakia (N = 451) found a similar pattern (p. 193).

Miquel-Feucht et al. (1999) based on a large study of 1400 Spanish individuals, claims that cribra orbitalia, cribra femora and cribra humeri have a shared aetiology. He goes as far as grouping them together in a 'cribrous syndrome'. However, more recent studies have not been able to support this idea (Schats, 2021, p. 87; Gomes et al., 2022, p. 1067).

2.5.2 Critique on using porous lesions as indicators of anaemia

In the 2000s, Wapler et al. (2004) argued against using cribra orbitalia as a clear indicator of anaemia. They applied both macroscopic identification methods for cribra orbitalia, as well as destructive histological analysis through polarized light microscopy on a collection of Nubian skulls. They showed that in only 43.5% of cases were cribra orbitalia was present, indications of anaemia could be found. The other 56.5% of cribra orbitalia cases without indications of anaemia could be subdivided into three groups, resulting from inflammation, post mortem erosion and other undefined signs. This study demonstrates the danger of identifying the condition based only on macroscopic methods, as well as the fact that other pathological conditions can mimic the appearance of cribra orbitalia.

Walker et al. (2009) challenge the widely accepted idea that iron-deficiency is the cause for porotic hyperostosis and cribra orbitalia. While the researchers agree that anaemia is the most likely cause for porotic hyperostosis, they explain that red bone marrow expansion actually requires stores of iron. It would therefore be very unlikely that this anaemia results from iron-deficiency. Instead, haemolytic and megaloblastic anaemias are found to be a much more likely cause. Megaloblastic anaemia manifests itself in the form of above normal sized red blood cells, which contain insufficient haemoglobin. The condition is most often caused by deficiencies of vitamins B12 and B9, the first of which is consumed through animal products and the latter through leafy greens (Srikanth, 2016). Walker et al. (2009) assert that malnutrition of mainly vitamin B12 was common in ancient populations and explains the high frequency of porotic hyperostosis in pre-Columbian societies in America. Because malaria was not present on the continent before European contact, these pre-Columbian societies would not have evolutionarily retained hereditary haemolytic anaemias such as thalassemia or sickle cell anaemia (p. 113). It is possible that iron-deficiency was common among these populations besides any B12-deficiency, but they say that this deficiency would not lead to hypertrophy and therefore not to porotic hyperostosis.

Walker et al. (2009) also explain that porotic hyperostosis does not necessarily have the same aetiology as cribra orbitalia, which would explain why they are most often found separately or why in some populations either porotic hyperostosis or cribra orbitalia is much more common. Instead of cribra orbitalia being an earlier stage of the same condition, the researchers claim that in many cases it is instead caused by the subperiosteal hematomas that can result from conditions such as rachitis, haemangiomas or even traumatic injuries, but mainly scurvy (p. 115). The orbital roofs of children have a higher density of veins between the periosteum and the bone underneath. This periosteum is also less firmly attached to the bone than in older individuals, which can be exaggerated when the connecting Sharpey's fibres are weakened through vitamin C deficiency (p. 116). According to Walker et al. (2009), this would explain why cribra orbitalia is almost never found in an active state in adult individuals (p. 116). Any slight trauma including movement of the eye muscles could cause subperiosteal bleeding, after which the blood cloths would be converted into highly vascular subperiosteal bone during the healing process (pp. 155-116). This additional bone can look identical to cribra orbitalia. They also mention clinical reports from the late 19th century where proptosis was often found in patients with scurvy because of the subperiosteal bone putting pressure on the eye ball (p. 115). Like Wapler et al. (2004) before, Walker et al. (2009) also consider factors that would amplify this system, such as high nutrient losses due to gastrointestinal infections resulting from bad sanitation.

Oxenham & Cavill (2010) refute the claim by Walker et al. (2009) that iron-deficiency anaemia cannot be considered a possible aetiology for porotic hyperostosis or cribra orbitalia due to a lack of marrow hyperplasia. They explain that while iron-deficiency anaemia does lead to a lower red blood cell count, this is the result of ineffective erythropoiesis whereby erythroblasts cannot form into working erythrocytes because there is not enough iron available. It is therefore wrong to equate the decreasing red blood cell levels with the inability of marrow expansion. In reality there is a major increase in erythropoiesis, albeit ineffective, which just like megaloblastic or haemolytic anaemia can lead to red marrow hyperplasia. Oxenham & Cavill (2010) do agree with Walker et al. (2009) that cribra orbitalia has a diverse array of aetiologies, but show that iron-deficiency indeed can lead to hyperplasia. The only type of anaemia where marrow hyperplasia is not the possible is anaemia of chronic disease (p. 199).

Rivera & Mirazon Lahr (2017) applied CT-scanning on a collection of crania belonging to young and middle aged adults from all across the world including Africa (N = 98). In this group, cribra orbitalia was found in 23 individuals. Each cranium was then subjected to 186 measurements of cranial thickness, dispersed over various lines across the surface connecting craniometric points (p. 79). It was shown that individuals with cribra orbitalia actually have significantly smaller diploe across the cranial midline and parietals that border it compared to those without cribra orbitalia (p. 92). They conclude that porotic hyperostosis and cribra orbitalia most likely have separate aetiologies. It is said that anaemia does remain the most likely cause for cribra orbitalia. While in cases where cribra orbitalia is associated with marrow expansion and/or porotic hyperostosis, hyperplastic anaemias such as iron-deficiency anaemia or haemolytic anaemias can still be considered the main cause. However, when it is related to diploic destruction, as is the case in this study, a hypoplastic anaemia should be considered. Rivera & Mirazon Lahr (2017) assert that the only hypoplastic anaemia that is common enough to account for the frequency of cribra orbitalia is anaemia of chronic disease. They do warn that scurvy can result in orbital lesions that are also disassociated from hyperplasia of the cranial vault and should therefore be considered as likely a cause for cribra orbitalia as anaemia of chronic disease.

One major problem with their study however is the large inter-population variance. After all, their study contained only 23 crania with cribra orbitalia which originated from wildly different geographic locations such as South-Africa, Sweden, Kenya, Sri Lanka, Australia or Peru, just to name a few. Each of these populations had wildly different climates, diets, parasites…etc.

Brickley et al. (2020) dedicates a full chapter of her book on metabolic bone disease in archaeology to anaemia. While she mentions the publication by Rivera & Mirazon Lahr (2017) and explains that there are types of anaemia that lead to marrow hypoplasia, she asserts that only marrow hyperplasia would lead to bone changes in cases of anaemia (p. 211). Brickley et al. (2020) puts emphasis on the complexity of anaemia and its many subtypes as well as the complex aetiologies of each kind. She produced a flow-chart for diagnosis in case porosity of the orbital roof is found. This chart contains an array of sequential steps based on either macroscopic, microscopic or radiological observation that help distinguish the cause as either anaemia or other conditions that can lead to orbital porosity such as scurvy, rickets, Paget's disease, trauma, ulcers or infection (p. 216). The main takeaway of her approach is that simple macroscopic evaluation is not enough because anaemia does not always produce porosity of the outer table of the bone, nor is every thickening of the cranial vault a sign of anaemia. When the whole structure shows thickening this is likely the result of Paget's disease of bone, when the thickening is due to deposition of new bone on top of the cortical bone it can be caused by an array of pathologies such as scurvy, rickets, neoplasia or infection. Only when diploic expansion can be observed and the structures are consistent with marrow expansion, anaemia can diagnosed.

2.5.3 Cribra orbitalia as anatomical variation

In their recent article however, Zdilla et al. (2022) propose a radically new interpretation of the phenomenon of cribra orbitalia. Unlike practically all previous research on the subject, they assert that cribra orbitalia is most likely not pathological in nature and can therefore not be used as a stress marker, nor as indication for any other kind of pathology. The researchers found that the presence of cribra orbitalia is significantly related to the presence of the meningo-orbital foramen. This meningo-orbital foramen, which has a whole array of alternative names, is defined as "a small opening in the orbit lateral to the lateral end of the superior orbital fissure" (O'Brien & McDonald, 2007, p. 880). Zdilla et al. (2022) explain that it is a non-metric trait, the frequency of which varies but is said to be more than 43% and in some studies even over 70% (p. 1632). They studied 78 adult and 12 sub-adult skulls (N = 90) and found that cribra orbitalia was present in 27.5% of individuals, while the meningo-orbital foramen was found in 65.8%. Most importantly, the researchers found that individuals with cribra orbitalia also had a meningo-orbital foramen in 91.4% of cases. On the other hand, crania with a meningo-orbital foramen do not have cribra orbitalia in 67.3% of cases (p. 1655). Furthermore, Zdilla et al. (2022) found that the orbital foramen and the cribra orbitalia are connected through vascular impressions (see Figure 5). In the three instances were cribra orbitalia was found but no meningo-orbital foramen, they attribute this to possible vasculature in other parts of the orbital roof, in one example there being a vascular impression between the cribra and the ethmoidal fovea (p. 1655). Zdilla et al. (2022) say that "Due to its typical location, cribra orbitalia likely represents a bony response occurring at the watershed region formed by the terminal arborization and anastomoses of vasculature coming from the posterior orbit (via meningo-orbital foramina), the medial orbit (via ethmoidal foramina), and the anteromedial orbit (via the supraorbital foramina/notches" (p. 1655).

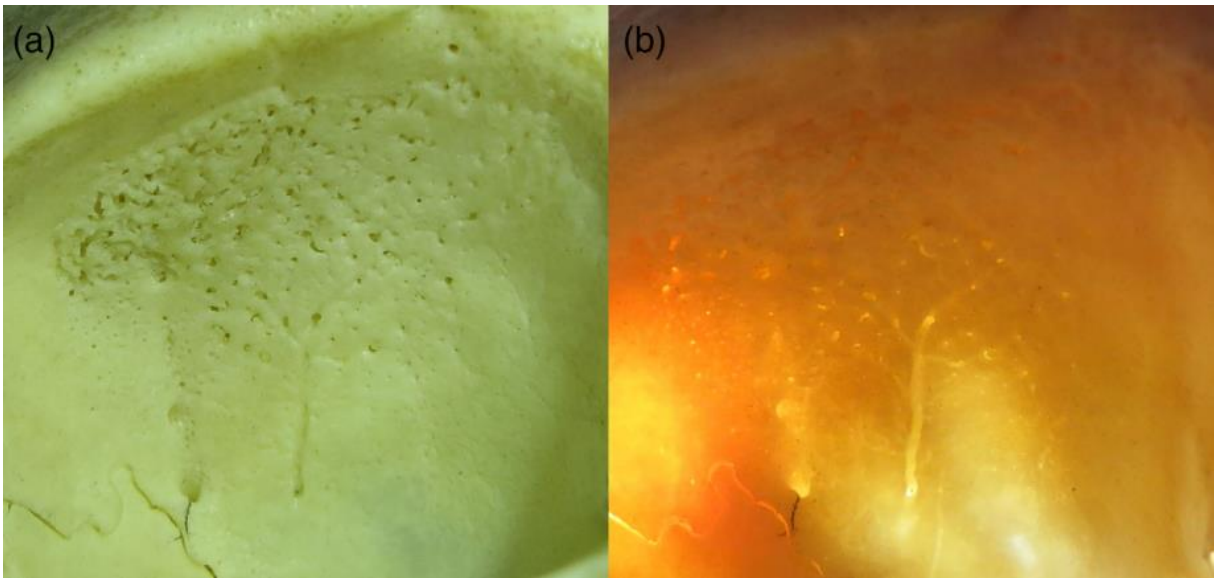

Figure 5: Cribra orbitalia and the meningo-orbital foramen. An eye orbit under standard lighting (left) and transillumination (right), showing a vascular impression that joins the cribra orbitalia with the concurrent meningo-orbital foramen. (Zdilla et al., 2022, p. 1634).

Zdilla et al. (2022) also review studies on modern populations with cribra orbitalia. The most important of these is the article of O'Donnell et al. (2020) who identified cribra orbitalia through post-mortem CT-scanning on sub-adults aged 0.5 to 15 years old (N = 490) who passed away in New Mexico between 2011 and 2019 (p. 1655). Cribra orbitalia was found to be present in 24.3% of individuals. Zdilla et al. (2022) argue against anaemia, scurvy, rickets or osteoporosis to be highly prevalent in a population from the modern United States. They conclude their article saying that the presence of a meningo-orbital foramen indicates a predisposition for cribra orbitalia, which is considered to be the result of

anatomical variation of the orbit vasculature, specifically the arteries that run through the meningo-orbital foramen (p. 1665).

When it comes to cribra femora or cribra humeri, they are often mentioned in discussions on the aetiology of porotic hyperostosis and cribra orbitalia but they are rarely, if ever, the main subject. This connection between cribra orbitalia and cribra femora is mostly based on similarities in appearance of the lesions, which is inherently dangerous. However, in their study of a medieval collection from North-Western Spain, Mangas-Carrasco & Lopez-Costas (2021) did find that cribra femora, cribra humeri and cribra orbitalia likely have a shared aetiology due to a similar healing pattern that was observed. Porotic hyperostosis was found to have a different aetiology (p. 169).

A rare study that looked specifically at cribra femora was carried out by Sealey et al. (2022) who used both macroscopic identification as well as CT-imaging to investigate a collection of 18th to 19th century sub-adults from Canada. They found strong correlations between the age or severity and the thickness of the anterior femoral neck. Because only limited evidence for marrow hyperplasia was found, the researchers were not able to define anaemia as the aetiology.

All things considered, we can say that there is no consensus on the aetiology of porous lesions. The list of possible causes that have been proposed over the last half century seems endless. However, the current debate has two major interpretations: on the one hand there is the idea best summarized by Brickley et al. (2020) in which porous lesions can result from one of multiple kinds of anaemia, as well as a hole array of other pathologies such as scurvy, rickets, Paget's disease or trauma. On the other hand, there is the theory by Zdilla et al. (2022) in which they say that cribra orbitalia is the result of anatomical variation of the vascularisation of the eye orbit and therefore most likely not pathological. The most recent studies also indicate that porotic hyperostosis may have a different pathology than the porous lesions it is often grouped together with.

2.6 The concept of portable X-ray fluorescence

This study explores the use of portable X-ray fluorescence (pXRF) in detecting the elemental composition of human bone material. The word 'portable' refers to the mobile aspect of this technique which allows the observer to move the pXRF-machine outside of a lab environment, unlike a normal XRF-machine which sits on a lab bench. In archaeology, this feature is useful as researchers can measure fragile or valuable objects in the museum or depot itself, without having to displace them. Both techniques are however based on the same concept: fluorescence (Bezur et al., 2020, p. 23).

In X-ray fluorescence, the individual atoms in a sample are put into an excited state by absorbing X-rays. The photoelectric effect determines that an X-ray photon can cause an electron on one of the inner shells of the atom to be expelled when it collides with it. The excited atom then restores its stability by having an electron from a higher shell take up its vacant position. Because this electron moves from a higher to a lower energy level, the law of conservation of energy determines that the excess energy must be lost. This is done in the form of a fluorescence photon that is emitted by the atom and subsequently detected by a sensor inside the XRF-machine (Forster et al., 2011).

Because each element has its own unique distribution of electrons over its shells, the emitted fluorescent photons each have their own energies. When the number of counts are plotted in a graph for each detected energy level, the different elements will form peaks. This allows XRF to distinguish the unique elements present in the sample. (see Figure 6) When taking into account the number of counts for each individual element, its is possible to determine the relative quantities of the elements

within the sample. In this study, we will use that feature to determine the concentration of elements like iron within the femora of the Middenbeemster and Arnhem collections (Bezur et al., 2020, p. 24).

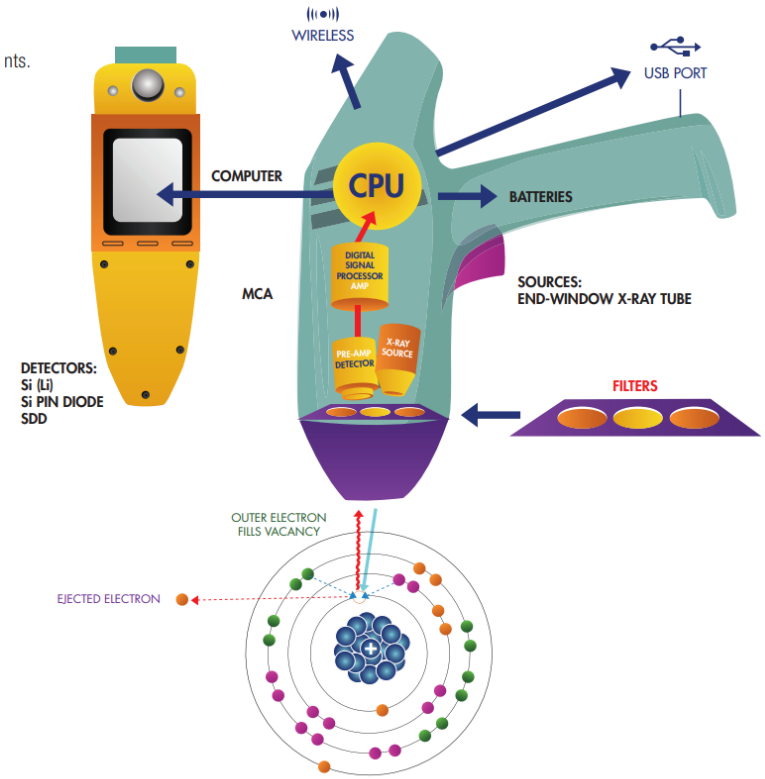

Figure 6: Portable X-ray fluorescence. A schematic overview of Portable X-ray Fluorescence. (Bezur et al., 2020, p. 23).

The main advantages of pXRF are the minimal preparation work of the samples and its non-destructive nature. Unlike lab based ED-XRF were the samples are damaged during preparation, a pXRF-machine can simply be fixed above an object (or even be handheld in the field).

Of course, there are a number of caveats that one needs to be cautious off. There are limits to the minimum dimensions that a sample needs to have in order to be scanned. Most types of pXRF are also not capable of measuring elements with an atom number below that of sodium (Na). Even when light elements like sodium or magnesium can be detected, their emitted energies are so small that they dissipate into the atmosphere very easily, especially when there is an air gap. The quantification of such elements are therefore significantly less accurate than those of heavier elements, like lead (Pb) (Forster et al., 2011).

The depth to which the X-rays penetrate into the sample is dependent on the energy settings it is operated at, as well as the density of the sample. In osteology however, there is usually the opposite problem with the bone in question being too large to fit inside the ED-XRF machine.

Regardless, the penetration depth usually does not extend a few millimetres. Yet Byrnes & Bush (2016), warn one should be careful when taking measurements on thin bones like ribs, as the penetration depth may extend past the cortical bone into the trabecular bone, which would affect the reading due to the high amount of air. They also mention the vulnerability of bone for diagenesis and environmental contamination. In one of their experiments, they measured different concentrations of strontium before and after sanding bones down. However, they consider cortical bone to be homogeneous in nature, while in reality it consists of osteons called Haversian systems, the walls of

which are in turn formed out of concentric lamellae (Clarke, 2008, p. 131). It is not explained to what extent this could have affected their readings, nor how deep the sanding went exactly.

2.6.1 The use of pXRF in Archaeology

In recent years, the use of pXRF in archaeological research has increased dramatically (Tykot, 2016). Lower acquisition costs have made the tool more accessible, while the accuracy and detection ranges of the pXRF-machines themselves have also been improved. This has resulted in a large number of publications on a wide range of different applications. pXRF has for example been used to examine periodical soil samples from an old floor level of a medieval house, allowing for the identification of different use areas within the house (Williams et al., 2021). Other scholars have used pXRF to determine the chemical make up of pigments on ceramics (Shoval & Gilboa, 2015) or even go as far as trying to distinguish different Attic black-figure painters through pXRF-analysis of pigments (Muskara & Kalayci, 2021). In short, there are endless ways in which pXRF can be used in archaeology and everyday month new applications and/or materials are published.

2.6.2 The use of pXRF in Human Osteoarchaeology

While pXRF has become more common practice in other branches of archaeology, its use within human osteoarchaeology has remained limited. Thus far, only a handful of publications have applied the technique on skeletal materials, most of which are from recent dates. McGarry et al. (2021) have demonstrated that bones of individuals retain their unique elemental compositions, even after heating to high temperatures. This could potentially allow for individuals to be identified within comingled cremation remains.

Kilburn et al. (2021) have used pXRf to determine the elemental concentrations of human bones and correlate these a number of pathologies such as rickets, scurvy, syphilis, porotic hyperostosis, smallpox and others. However, due to the small sample size, many of these conditions are only present once. Many of the individuals under study also suffered from multiple pathologies, making it hard to isolate variables. The claimed correlations therefore seem not very meaningful. Besides this, there are other methodological problems with this study, such as the tendency to use completely different types of bone when the standard bones for measurement were not available, without regard for differences in elemental concentrations or thickness of the cortical bone. Traditional industry near the graveyard from which the bones originated also affected the material, as can be seen from the high readings of titanium and aluminium.

Zdral et al. (2021) have combined pXRF of human bone material with Dual-Energy X-ray Absorptiometry (DXA) to study osteoporosis in skeletal remains of adult females from Coimbra. They found that the concentration of phosphor (P) is lower in adults over the age of 50 than those below it, meanwhile the concentration of sulphur (S) and the calcium/phosphor-ratio were found to increase in this age group.

Finally, Gomes et al. (2021) used pXRF to examine elemental concentrations of individuals with anaemia as known cause of death. A group of male and female individuals with this cause of death was selected, as well as a control group. Both groups were then checked for cribra orbitalia and porotic hypostosis, before each skeleton was measured through pXRF. One can however ask questions about the accuracy of the anaemia diagnosis as cause of death in the early 20th century.

Human osteoarchaology has been slowly catching up with the use of portable X-ray fluorescence spectrometry compared to other branches of the archaeological field. As of yet, the number of publications is still quite limited. Possibly, the current study could be able to contribute to this emerging field and help in developing protocols for pXRF-measurements of human remains.

2.7 Previous pXRF-set up's

Because the use of pXRF in osteological research is still quite new, there has not yet been developed a standard method for positioning the bone relative to the machine. As a result, there is wide variation in techniques between scholars, each with there own unique advantages and disadvantages in regards to speed, safety and ease of use. Perrone et al., (2014) mount the pXRF-machine in its holder with the sensor facing upwards and balance the bone on top of it (see Figure 10). This allows for a fast sequence of measurements, because the machine itself does not need to be repositioned after each sample. One can simple take the bone of the sensor and replace it with the next bone. There are however a number of major disadvantages with this technique: there is direct contact between the bone surface and the fragile membrane that seals of the vacuum tube, which could cause damage to it. Secondly, with the bone balancing on the upward facing end of the pXRF-machine, there is considerable risk of the bone falling off and getting damaged in the process. It will also be quite difficult to correctly position any bone that are asymmetrical due to post mortem damage or abnormal shape.

Figure 7: pXRF set-up by Perrone et al. The bone is balanced on top of the sensor. (Perrone et al., 2014, p. 151).

(Henderson 2019, pp. 28-32) follows a similar technique, but solves some of the abovementioned problems regarding the falling hazard and asymmetry by securing one end of the bone to a retort stand with a utility clamp (see Figure 11). However, in this method the bone surface still makes direct contact with the sensor membrane. Given the rounded shape of most human bone material, the escape of some radiation during measurements is unavoidable. It is therefore safer to have the pXRF-machine in a downward facing position. The mounting stands that position it in an upwards position (and which often get delivered with the machine itself) are meant to be used in combination with a platform that slides over the front of the pXRF and a round cap that stands over it. Both are made with dense metal, which essentially creates a radiation proof chamber from which little to no X-rays can escape. This is

not the case when measuring large bones without the cap. The pXRF should therefore be facing downwards so that most of the escaping or reflecting radiation is absorbed by the table, rather than being dispersed into the room.

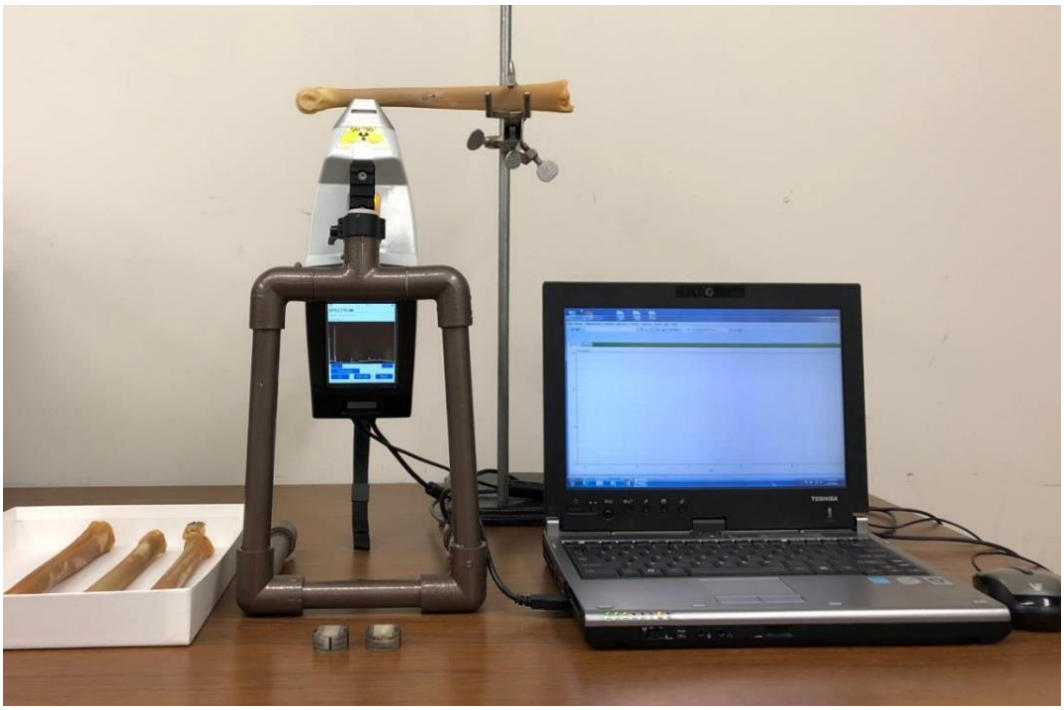

Figure 8: pXRF set-up by Henderson 2019. The bone is balanced on top of the sensor, but with additional support. (Henderson, 2019, p. 30).

(Zdral et al., 2021, p. 233) make use of a custom V-shaped stand with a coating that is both flexible and adaptable, in order to secure femora in place (see Figure 12). The measurements are then carried out in a downward facing position from a handheld pXRF-machine. This seems to be an improvement over the methods of Peronne et al. (2014) and Henderson (2019), in particular by measuring in a top down position and therefore not resting any weight on the sensitive sensor. The securing stand works well for the aim of this specific study which only took measurements of femora at midshaft, but will likely be less suited for studies that require the measuring of different bones or bones that are abnormally shaped due to certain pathological conditions, for example a tibia with severe bending due to rachitis.

Even though the X-ray source is facing downwards, it is not advisable to use the machine in a handheld way because some radiation will still escape. While the energy levels are only a fraction of those in for example an roentgen image, the exposure time is much longer (up to 180 seconds per measurement at Zdral et al. (2021)). With most studies consisting of a whole array of measurements, it is better to attach the pXRF-machine to a tripod with adjustable height. This way, a sufficient distance can be created between the observer and the radiation source. Besides these safety improvements, attaching the machine to a tripod also benefits measurements. This is because the exact position of the machine as well as the minute distance between the sensor membrane and bone surface remain locked during the (often relatively long) measurement, without added tremor from the observer.

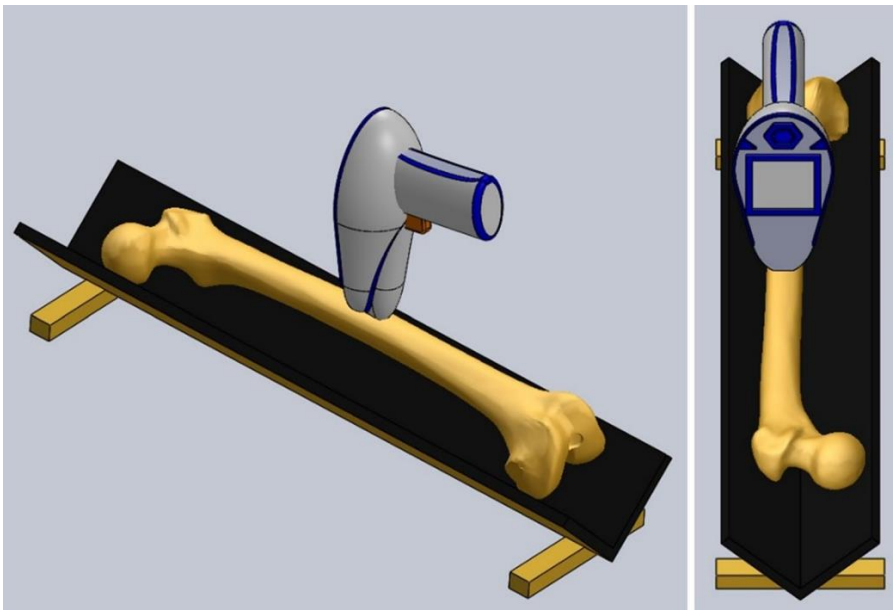

Figure 9: pXRF set-up by Zdral et al. The bone is placed in a V-shaped support and measured in a top-down position. (Zdral et al., 2021, p. 233).

These discussed pXRF-set-up's will serve as a basis to develop our own pXRF protocol that fits with our research aims, while also taking into account practical and safety considerations. This new protocol will be discussed in detail in the methods chapter further below.

2.8 Archaeological context

Before we discuss the study of skeletons from the Middenbeemster and Arnhem osteological collections, it is important to discuss the archaeological background of either site. Below, we will give a summary of the location, specific burial practices and graveyard history of the burials at the Keyserkerk in Middenbeemster and Saint Eusebius Church at Arnhem.

2.8.1 The Keyserkerk at Middenbeemster

The individuals that belong to the Middenbeemster osteological collection at Leiden University, originate from the protestant Keyserkerk in the village of Middenbeemster, which is located in the Dutch province of North Holland (see Figure 7) The village is located on a polder, which is an artificially drained piece of land, common across the Netherlands. Plans for the construction of a new reception area with toilets at the Keyserkerk would disturb many of the hundreds of burials on the church ground (Hakvoort 2013, 11-15). A collaboration of commercial archaeologists from Hollandia NV and archaeologists from Leiden University carried out extensive excavations during the summer of 2011. In total, 412 individuals were excavated at the site. They have each been washed and are currently stored in the depot of the Laboratory for Human Osteoarchaeology at Leiden University, were they form an important research collection (Van Nuland, 2019).

Based on the archaeological finds that were interspersed with the burials, it was determined that the general population at Middenbeemster belonged to the middle class. The construction of the Keyserkerk starts in 1616, which forms the starting point of burials at the site. However, in 1829 the town administration of Middenbeemster buys the church graveyard with the aim of turning it into an

official town graveyard. During this process, the original burials at the graveyard were removed. In 1867 a new town graveyard is put into use, after which burials on the church grounds were outlawed (Hakvoort 2013, 29). This gives a dating between 1829 and 1867 for the majority of skeletons that were excavated at Keyserkerk, although some can go back as early as 1615. Individuals were usually buried inside wooden coffins, in one case with their name, age and date of death spelled out with nails on the coffin lid (Hakvoort 2013, p. 31-33).

Economically, the Middenbeemster population was based on farming, originally agriculture but when that was found not to be successful, they switched to dairy farming which remains important until the current day.

The human remains at the site were found to have been well preserved. DNA was sampled from teeth of a number of individuals (Hakvoort, 2013, pp. 19-20).

A selection of 125 individuals was made by Leiden University that contained adult males, females and sub-adults. These skeletons were subjected to more detailed osteological study, which was published as part of the archaeological report of Hollandia NV. In this first study, a number of important insights into the health at 19th century Middenbeemster were discovered. The graveyard yielded relatively many sub-adults, although this can possibly be attributed to the good state of conservation, rather than Middenbeemster having a higher child-mortality than other regions at the time (Lemmers et al. 2013, p. 48). Linear enamel hypoplasia was found to be present in 43.5% of sub-adults, indicating that they suffered stress during their youth (Lemmers et al., 2013, p. 49-50). This could be sickness, malnutrition or a combination of both during the development process of a tooth, temporarily disrupting the production of enamel which results in a banded pattern on the crown of the teeth.

Cribra orbitalia was observed in four individuals or 5.9% of the selected skeletons, but the authors demonstrate that these frequencies can vary greatly between archaeological contexts (Lemmers et al., 2013, p. 53-54). In the report, no mention is made of the frequency of cribra femora.

Figure 10: The Middenbeemster site. A burial at Middenbeemster (left) and the excavation next to the Middenbeemster church (right). (Hakvoort, 2013, p.30).

2.8.2 The Saint Eusebius Church at Arnhem

The second osteological collection used in this paper consists of burials at the Saint-Eusebius Church in the city of Arnhem, which is located in the province of Gelderland in the east of the Netherlands (see Figure 8 & 9). The Sint-Jans Creek runs throughout the city but, like many open water ways at the time, it was closed off in the 19th century. The city of Arnhem decided to reopen this creek as part of its efforts in making the city centre more green. These construction works also necessitated the moving of underground cables and sewage pipes. In 2017, the commercial archaeological company RAAP started excavation of a 700m long section of the Sint-Jans Creek through multiple streets in the city (see figures 8 & 9). The middle part of this route consists of the Kerkplein in front of the Saint Euseubius church, as well as the Boerenstraat which forms the area directly north of the church. During this large excavation project, many hundreds of skeletons were found in the vicinity of the Saint Eusebius church (RAAP bv., 2017).

Construction of the Saint Eusebius church commenced in 1452 and was built in late Gothic style (Eusebius Arnhem, 2023). The skeletons in the Arnhem osteological collection at Leiden University can therefore be dated from the Late Medieval Period all the way up to the 19th century. They should be considered members of quite low economic class who lived in an urban context. This low economic standing is also indicated by their burial on the North side of the church, as well as the very simple burials themselves (RAAP bv., 2017).

The city of Arnhem had a modest population until the late 18th century, after which the population grew exponentially during the 19th century (Volkstellingen, 2022). Most inhabitants were originally involved in trades, but during the 19th century the city developed a strong industry. These two aspects combined, mean that most of the lower class population lived in overcrowded neighbourhoods with bad sanitation.

2.8.3 Comparison of both archaeological contexts

We can see that both osteological collections used in this study have quite different backgrounds: while the Middenbeemster skeletons represent a rural village near the Zuiderzee in the West of the Netherlands, the remains from Arnhem originate from an urbanized context in the Eastern part of the country. Besides the geographical difference, the collections also represent historical differences with Middenbeemster being almost exclusively dated to the 19th century, while the Arnhem material is often much older. Finally, both archaeological sites represent different socio-economic realities, with the Arnhem burials being of a generally lower economic class than those at Middenbeemster.

These historical and economical differences likely represent differences in diet as well, with a sea-side town like Middenbeemster possibly consuming more fish and sea-food than a city population of low economic standing such as Arnhem. Diets at Arnhem were likely also lower in meat than a rural middle class context like Middenbeemster, leading to a lower iron intake at Arnhem. Such dietary differences could lead to differences of elemental concentrations in the skeletons. Besides this, the differences in soil between the two sites could also affect the elemental concentrations. The pXRF-measurements of both sites will later on in this thesis be compared to see if there are statistically significant differences in elemental concentrations between them.

Figure 11: Excavation of a skeleton at Arnhem. (RAAP, 2017).

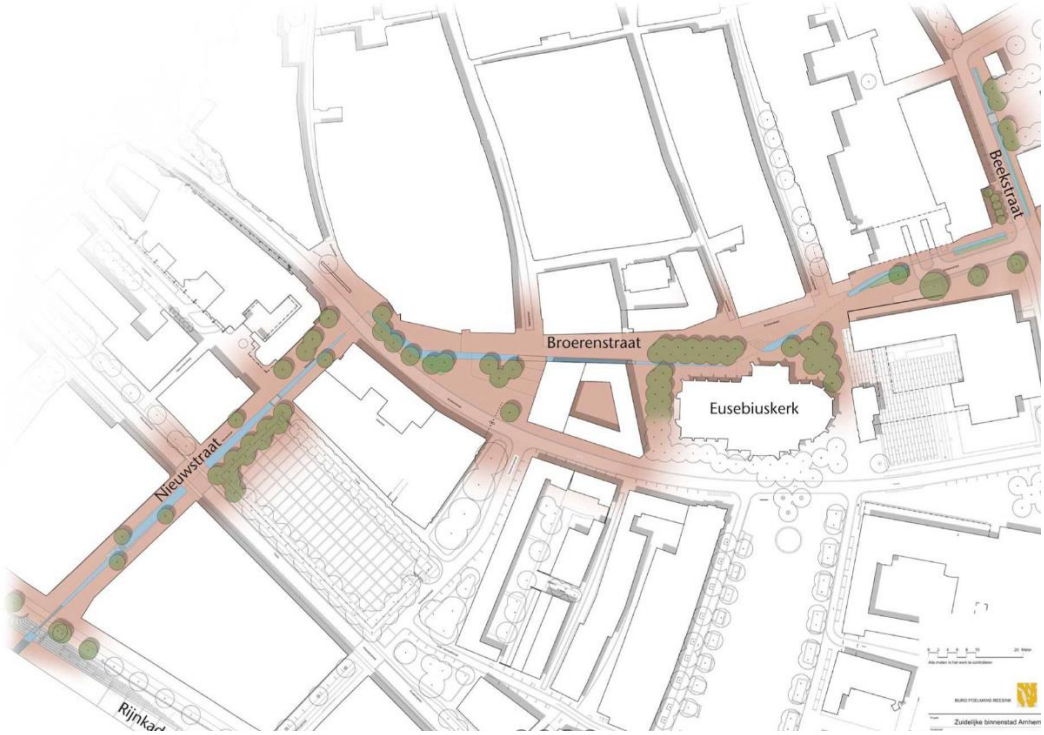

Figure 12: Excavation lay-out. Plan of the Arnhem city centre surrounding the Eusebius church, excavations were carried out in the area marked red. (RAAP, 2017, https://www.raap.nl/magazine/RAAPMAGAZINE201702/index.html#extFeatures9-2).

In the following chapter the materials used for study in the current paper will be introduced, namely selected samples from the Middenbeemster and Arnhem osteological collections at Leiden University.

3: Materials

In this chapter we will introduce the skeletons that were studied through portable X-ray fluorescence, how they were selected and how their sex and age-at-death were determined. This information is summarized in tables 1 and 2 further below.

The skeletal remains that were selected for the current study include both adults and sub-adults from the Middenbeemster and Arnhem osteological collections at Leiden University. During the yearly internship program at the Laboratory for Human Osteoarchaeology, students individually assess the sex, age-at-death and estimated height, followed by a full pathology report of a number of skeletons. These reports are then checked by senior members of the laboratory and made available for study. The skeletal remains in the Middenbeemster and Arnhem collections have each resulted from the internship program. A variety of methods is used by the students for their assessments: In adults, the age-at-death is determined through dental attrition (Maat, 2001), the auricular surface (Buckberry & Chamberlain, 2002), suture closure on the ectocranial surface (Meindl & Lovejoy 1985), the pubic symphysis (Brooks & Suchey, 1990) and the sternal rib ends (Iscan et al., 1986). Sex was not determined in sub-adults because the traits used for sex determination have too much overlap in this group, causing a large risk on wrong identification of sex. In adults however, this was assessed using traits of the cranium, mandible and pelvis according to the method of Buikstra & Ubelaker (1994), as well as the method of the WEA by Ferembach et al. (1980).

No infants were included in the current study. Five distinct age groups were defined: Children (ages 3 – 12), Adolescents (13 – 18), Young Adults (19 – 35), Middle Adults (35 – 49) and Older Adults (50+). All sub-adults from Middenbeemster and Arnhem that have been processed up to the current day (meaning age-at-death has been determined) have been included, while for the adult individuals selections were made.

In the case of the Middenbeemster adults, the skeletons that were selected are those that were identified as having cribra femora in the student pathology reports. A number of other adult skeletons with at least one intact femur were then selected randomly from the Middenbeemster collection in order to form a control group with which the cribra femora group could be compared. The adult skeletons of Arnhem resulted from the random selection of 25 individuals with at least one intact femur. This means that not every selected individual is guaranteed have at least one intact eye orbit, especially in the case of sub-adults.

Because the collection of the Middenbeemster adult group is not random, no statistical interpretations regarding frequency will be made for the Middenbeemster adults. To this end, only the sub-adults from both sides and the adults from Arnhem will be used to study frequency of cribra femora because they represent a random selection. However, the Middenbeemster adults do offer the advantage of having a large number of individuals with cribra femora present to compare with the non-cribra femora control group when analysing the elemental compositions.

The number of selected individuals for each of the four groups, together with their break down into sex and age groups can be found in the tables 1 and 2 below:

Table 1: The selected adult skeletons per age-at-death group. (Figure by Martijn Jacobs).

Collection	*Female Younger Adults*	*Male Younger Adults*	*Female Middle Adults*	*Male Middle Adults*	*Female Older Adults*	*Male Older Adults*	*Total*
Adults Anrhem	6	3	3	8	1	4	25
Adults MB	3	3	2	3	3	4	18

Table 2: The selected sub-adult skeletons per age-at-death group. (Figure by Martijn Jacobs).

Collection	*Children*	*Adolescents*	*Total*
Sub-adults Middenbeemster	26	10	36
Sub-adults Arnhem	3	10	13

Currently, no soil samples from the Middenbeemster or Arnhem sites are present at Leiden University. They could have been used to determine the elemental composition of the soil in which the individuals were buried and compare this with the measurements of the bones, to see if there has been contamination by the soil.

4: Methods

For every individual under study a measurement was carried out through portable X-ray Fluorescence on the left femur. If no left femur was available or measurements were not possible due to post mortem damage, this was substituted with the right femur of the same individual. At least one intact femur was needed for and individual to be included in the sample.

In addition to the pXRF-measurements, every individual was macroscopically checked for cribra femora on the femoral neck and cribra orbitalia inside the eye orbits, using the method of Wapler et al. (2004) for cribra orbitalia and Mangas-Carrasco & lopez-Costas (2021) for cribra femora. The size of the porotic lesions was not indicated, scoring only their presence or absence.

4.1 Current pXRF set-up

In the background chapter, various pXRF set-up's of other scholars have been evaluated. Based on these evaluations, a new method for pXRF set-up was developed that best fits the specific research aims while taking into account practical and safety considerations.

The method used in the current study can be seen as a further development of the method by Zdral et al. (2021). Here, the femora were placed in a horizontal position on a flat surface, supported by a number of synthetic sponges of various sizes (see Figure 13). The sponges serve a dual purpose, they project the bone against the hard surface of the underlaying table and stabilize it in the preferred position. Because of the size difference of the sponges, the shape of bone itself becomes irrelevant. Any bone can be easily positioned to have a relatively flat area pointing upwards to the sensor, even in cases where the bone has a challenging geometry. Next, the pXRF-machine is mounted in a downward-facing position to a tripod that has a lever to slowly lower the machine down towards the surface of the femur, as well as a lever for backwards and forwards movement. This way the pXRF-machine can be accurately moved in all three degrees of freedom, without having to touch the machine itself. A built-in camera in the tip of the pXRF-machine helps in aiming the tip exactly at the point of interest.

In order to minimize the diffraction of the induced radiation, a gap of less then one millimetre was created between the bone surface and the membrane that seals of the vacuum tube. It is not advisable to make direct contact with the surface, as this could damage the delicate membrane which would render the machine inoperable. The air gap between bone surface and membrane mainly affects the lighter elements because their smaller energies dissipate more easily, which can be seen in much lower readings for the element calcium.

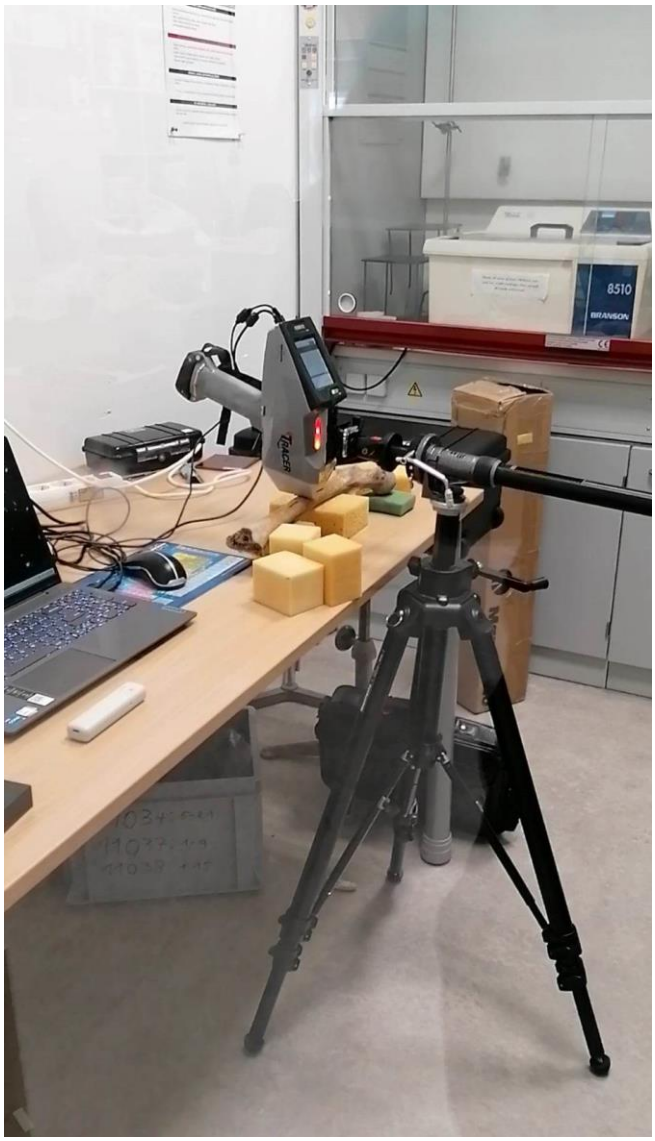

Figure 13: pXRF set-up in the current study. The bone is scanned in a top-down fashion by a pXRF supported on a tripod. (Photograph by Martijn Jacobs).

4.2 Measurement locations

Originally, the aim was to measure each femur both at Midshaft (MS) and the Femoral Neck (FN), as Zdral et al. (2021) had shown a few statistically significant differences in the elemental concentration of each location. A higher ratio of Ca/P was found at the femoral neck and an increased concentration of P, S, Ca and Zn at midshaft respectively (Zdral et al., 2021, p. 234). This could perhaps be related to differences in thickness of cortical bone at either location.

In practice however, it was in many cases not possible to do pXRF measurements at the femoral neck. The tip of the Bruker Tracer 5g was often too wide to fit in between the femoral head and the intertrochantric crest. In combination with the stronger curvature of this area, this meant that is was often not possible to achieve a gap of one mm or less with the bone surface, sometimes even reaching 5 to 10mm in size. Every extra millimetre of air between the sensor and bone surface is exponentially more problematic as more energy gets dissipated. Zdral et al. (2021) used a different pXRF-machine than the one in the current study (the Thermo Scientific Niton XL3t 900 GOLDD+ vs the Bruker Tracer 5g), but these seem to have roughly equal dimensions. The authors do not mention how they overcame

this problem or if they simply discarded femora where this is the case from their dataset (something that would negatively affect juvenile and female femora, as they have smaller necks).

The femoral neck is also more prone to post mortem damage and has a rougher surface, once again increasing the amount of air between sensor and bone surface. For consistency, it was therefore decided to only do measurements at the midshaft of each femur.

This is not to say that measurements at midshaft are without problems: the roundness of the diaphysis has a negative relationship with the size of the femur, meaning that the smaller the bone gets the rounder its surface. As the X-ray beam has a cross-section of 8mm, the more curvature there is within this area, the more diffraction will take place. When analysing the spectra, one should consider this bias of lesser accuracy towards smaller individuals, especially when working with juvenile material.

4.3 Safety

For reasons of safety as well as to decrease wear and tear, the pXRF-machine is not operated directly through its touchscreen, but instead is controlled remotely through the Bruker Remote Control software. A radiation meter would always be present during measurements and has a built in alarm that goes off if unsafe levels of radiation are detected. For matters of safety redundancy, the observer would always leave the lab during measurements of the pXRF.

4.4 Sample preparation

Although the skeletal remains in both the Middenbeemster and Arnhem collections have been thoroughly washed after their excavation, dirt stuck into bone crevices or sections of damaged bones may still affect the surface of bones that are kept in same plastic bag. While this is likely a minor issue, some scholars choose to clean the measurement area of each bone with 100% ethanol (Perrone et al., 2014, p. 150). This could however be harmful to the bone, thereby rendering the main advantage of using pXRF (its non-invasive nature) useless. Instead, the measurement of the bones in this study were rinsed with distilled water and dried with a clean synthetic sponge.

4.5 Calibration

The Bruker Tracer 5g does not yet have a dedicated calibration for the study of bone material, forcing the researcher to use an alternative setting that will perform well in quantifying the concentrations of the elements of interest in the bone. This inconvenience of not having a specific calibration for bone is also present in other brands of pXRF such as the Thermo Scientific Niton, with most scholars operating the machine in Mining mode (Kilburn et al., 2021, p. 3; Zdral et al., 2021, p. 237). In this paper however, it was decided to operate the pXRF in Mudrock Air mode. This calibration setting has been developed for the study mud of rocks and related materials, the “Air” specifying that it is used in an open air atmosphere, as opposed to a helium atmosphere. It measures sodium (Na) up to uranium (U) in two 45-second cycles, one aimed at lighter and one at heavier elements, for a total of 90 seconds per measurement. In the future, there are possible plans for Leiden University to acquire a human bone standard that would allow us to create our own dedicated calibration for bone materials.

4.6 Software

The generated PDZ-files are transferred from the machine and split into the two separate spectra using the Bruker CalToolkitEC software, which were subsequently loaded into the Bruker Artax software (version 8.0.0.476). This allows the spectra to be visualized and graphically compared with each other. The exact elemental concentrations of each measurement are written down by the machine into a csv-file. These data were then analysed using GraphPad Prism version 9.5.1.733.

4.7 Data analysis

The Mudrock Air-calibration measures the following elements: Na, Mg, Al, Si, P, S, Cl, K, Ca, Ti, V, Cr, Mn, Fe, Co, Ni, Cu, Zn, Ga, As, Sr, Rb, Y, Zr, Nb, Mo, Ba, Pb, Th and U. However, when the concentration of an element within the population is so low that 50% or more of the measurements were below the Bruker Tracer 5g's detection limit, the element in question was removed from the current study. This was done to avoid the small group of measurements above the detection limit to cause an overestimation of the actual concentration in the population. In this case, the selected elements are Na, Mg, Al, Si, P, S, K, Ca, Ti, Mn, Fe, Cu, Zn, As, Sr, Pb.

For both the Middenbeemster and Arnhem samples, each of the selected elements were checked for normality graphically through QQ-plots and formally by using the D'Agostino & Pearson test. This will determine whether parametric or non-parametric tests need to be used during the analysis. When a Gaussian distribution is present in both comparison groups, an unpaired student's t-test is used and if this is not the case instead the non-parametric Mann-Whitney U test. Descriptive statistics are used to explore the dataset, as well as calculate means, standard deviations and ranges.

Fisher's exact test is used to determine if cribra femora is significantly more frequent in males or females. The same analysis is used to determine if the condition is significantly more frequent among adults or sub-adults. When Firsher's exact test yields a significant result, the odds ratios are calculated using the Baptista-Pike method. All statistical calculations are done in GraphPad Prism version 9.5.1.733.

5: Results

5.1 Macroscopic results

The first step in analysis is to compare the relative frequencies of cribra femora and cribra orbitalia for each of the age groups. This yielded the following graphs below. A downwards trend in frequency can be observed as the age-at-death increases in both Middenbeemster and Arnhem (see figure 14 & 15). An immediate difference between both sites can be seen in the relative proportions of cribra femora and cribra orbitalia. At Middenbeemster, the frequency of cribra orbitalia is roughly half that of cribra femora, meanwhile in Arnhem both frequencies are very similar across the age groups.

Another notable difference is that at Middenbeemster, the frequency of cribra orbitalia is near stagnant from children up to middle adults. Each of the three adult groups also has frequencies that are much higher than those in Arnhem. However, as mentioned before, the sampling of the adult group at Middenbeemster was not done randomly but based on previous diagnosis of cribra femora in their associated pathology reports, with some added controls. This likely explains the inflated frequencies of cribra femora for these age groups in the Middenbeemster graph. Even with these inflated cribra femora frequencies, the cribra orbitalia frequencies at Middenbeemster are also higher than those in Arnhem.

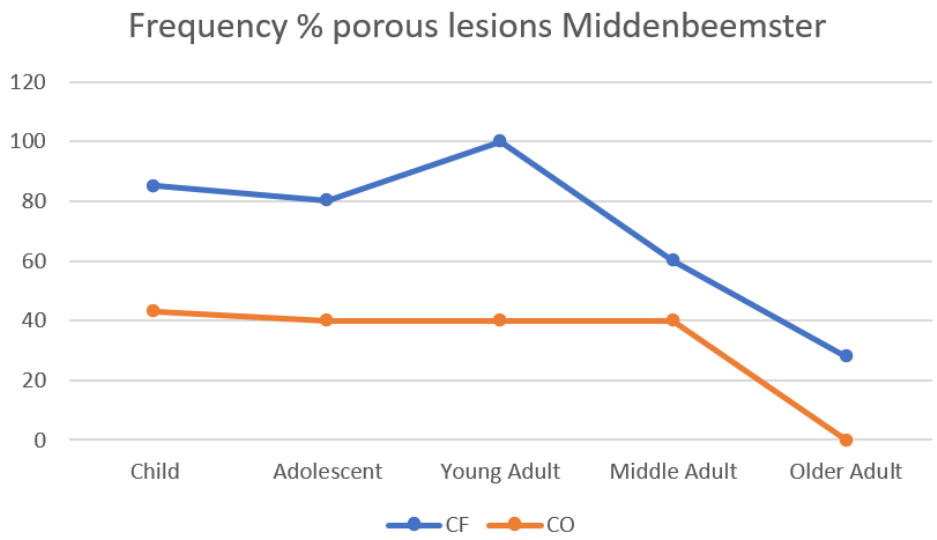

Figure 14: Percentage frequency of porous lesions in Middenbeemster. (Figure by Martijn Jacobs).

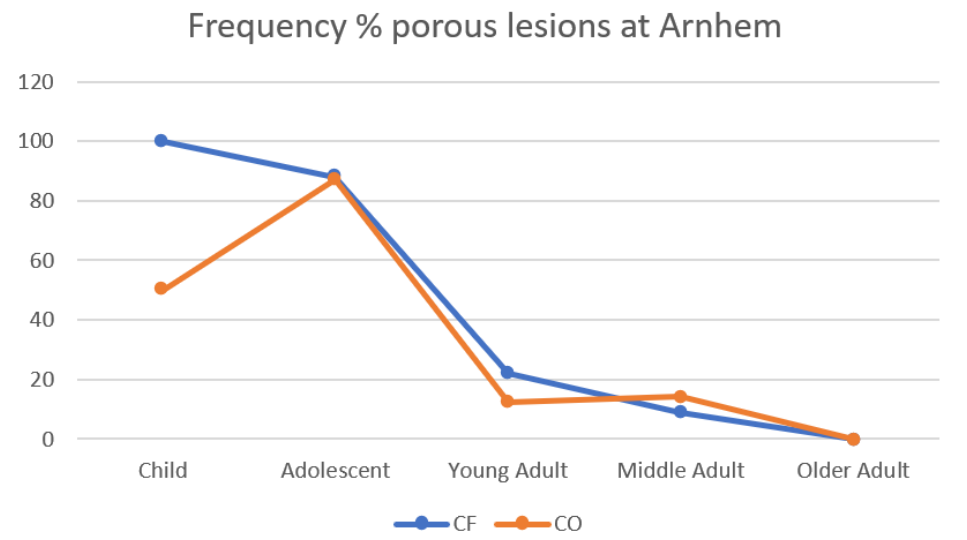

Figure 15: Percentage frequency of porous lesion in Arnhem. (Figure by Martijn Jacobs).

A Fisher's exact test was applied to investigate any possible relationships between age-at-death or sex with the presence for cribra femora. This yielded the following results (see table 3 to 6), although no statistically significant P-values were found for the first two tables, likely due to the relatively small sample sizes.

Tables 3 and 4 are contingency tables of Middenbeemster and Arnhem respectively that compare individuals with and without cribra femora against sex. Because no sex determination is done for sub-adults, the sample sizes are quite small, 17 individuals for Middenbeemster and 25 for Arnhem. The Fisher's exact tests did not yield statistically significant p-values, although Arnhem came close. Cribra femora therefore is not more present in either one of the sexes.

Table 3: Individuals from Middenbeemster with and without cribra femora per sex. (Table by Martijn Jacobs).

Data analyzed	No cribra femora	Cribra femora total	Total
Male	5	5	10
Female	2	5	7
Total	7	10	17

Fisher: P-Value = 0.6221

Tabel 4: Individual from Arnhem with and wihtout cribra femora per sex. (Table by Martijn Jacobs).

Data analysed	No cribra femora	Cribra femora total	Total
Male	15	0	15
Female	7	3	10
Total	22	3	25

Fisher: P-Value = 0.0522

Tables 5 and 6 are contingency tables of Middenbeemster and Arnhem respectively that compare individuals with and without cribra femora against adults and sub-adults. Because of the non-random sampling of the Middenbeemster adults, table 5 will be ignored as its adult cribra femora values are inflated.

Fisher's exact test of table 6 yielded a significant p-value. This means that sub-adults are statistically more likely to have cribra femora. In order to quantify this increased change, the odds ratio was calculated with the Baptista-Pike method. This yielded an odds ratio of 0.02479 and reciprocal odds ratio of 40.33. This means that sub-adults at Arnhem have a chance of cribra femora that is 40 times higher than adults from the same site.

Table 5: Adult and sub-adult individuals from Middenbeemster with and without cribra femora. (Table by Martijn Jacobs).

Data analysed	No cribra femora	Cribra femora total	Total
Sub-adults	6	31	37
Adults	7	11	18
Total	13	42	55

Fisher: P-Value = **<0.0001**

Odds ratio = 0.3041, reciprocal odds ratio = 3.288

Table 6: Adult and sub-adult individuals from Arnhem with and without cribra femora. (Table by Martijn Jacobs).

Data analysed	No cribra femora	Cribra femora total	Total
Sub-adults	2	11	13
Adults	22	3	25
Total	24	14	38

Fisher: P-Value = **<0.0001**

Odds ratio = 0.02479, reciprocal odds ratio = 40.33

5.2 Elemental composition analysis

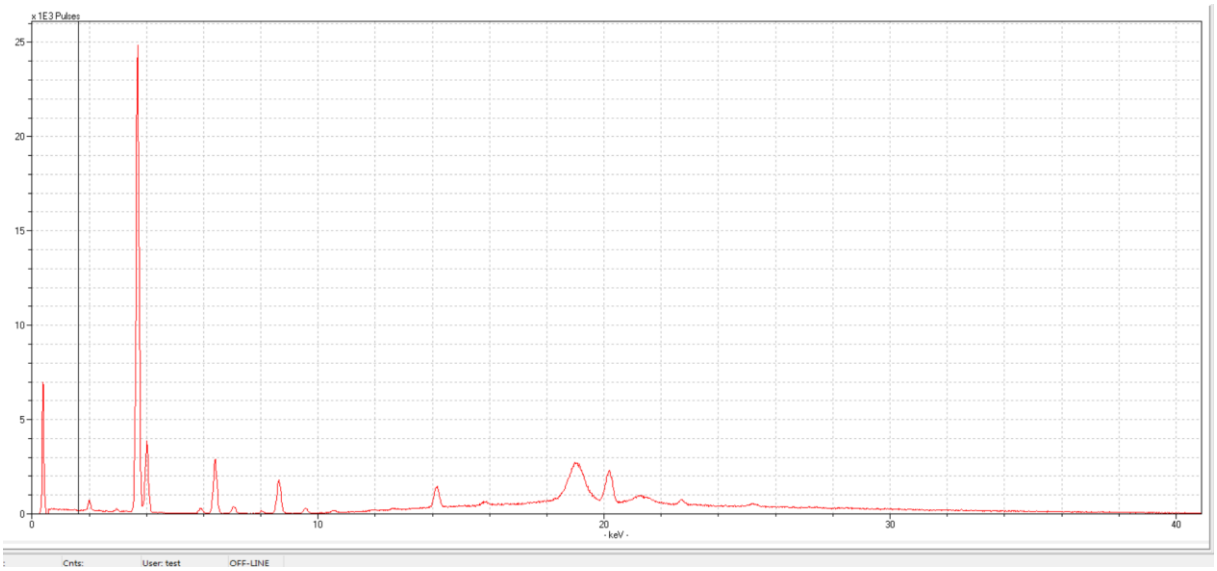

Figure 16: pXRF-sepctrum. An example of an XRF-spectrum, taken from the left femur of skeleton S404V548). (Figure by Martijn Jacobs).

A box and whisker plot was used to inspect the combined dataset the contains both the Middenbeemster and Arnhem data. Because of the large variations in concentration between some elements, a Log10 scale was applied. Two QQ-plots were then generated for Middenbeemster and Arnhem and then mathematically tested through the D'Agostino & Pearson test with alpha = 0.05.

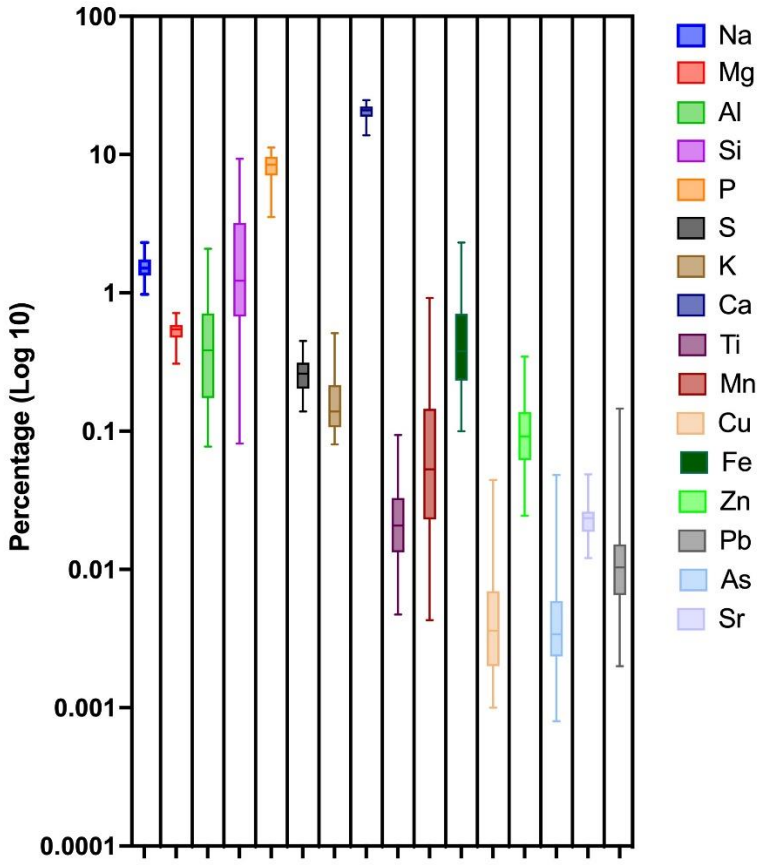

Figure 17: Elemental concentrations. Box and whisker plot (on scale Log 10) of the combined data from Middenbeemster and Arnhem. (Figure by Martijn Jacobs).

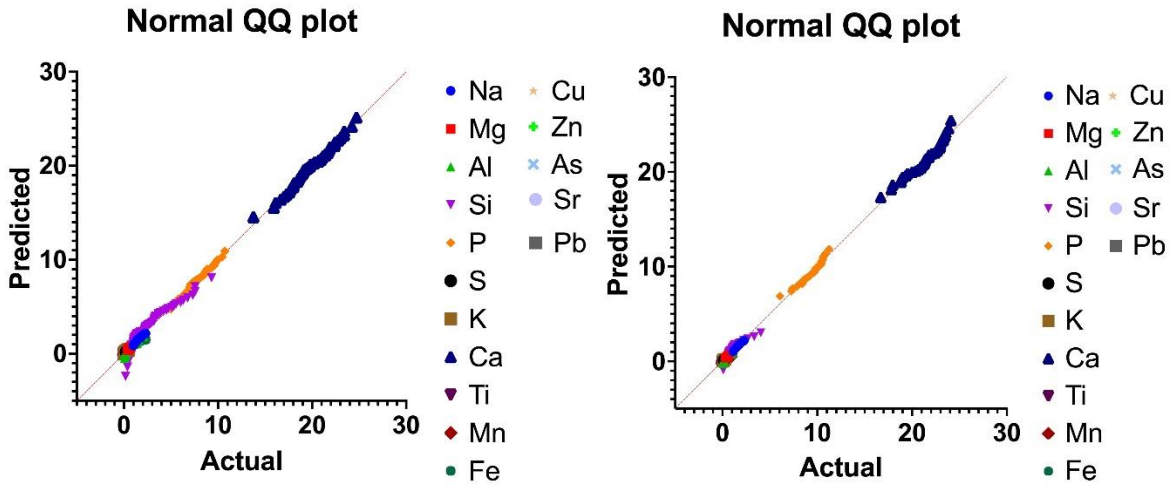

Figure 18: Normality check. Normal QQ-plots of Middenbeemster (left) and Arnhem (right). (Figures by Martijn Jacobs).

The first and foremost analysis was to compare the elemental concentrations between Middenbeemster and Arnhem. Given the geographical distances between both locations, it can be hypothesized that at least some of the elements will have a significantly different concentration. However, if no significant differences are found, this would indicate that the skeletal remains have not

been altered by diagenesis and that the larger combined dataset can be used, instead of calculating identical analyses for either location.

The resulting table (7), shows that there is a significant difference in concentration between both sites for the majority of elements under study. A scatter dot plot was used to illustrate this graphically (see figure 19). Only four elements (Na, Ti, Mn and Cu) did not show a significant increase or decrease in concentration. Based on this table, it was determined that datasets with elemental concentrations of Middenbeemster and Arnhem could not be combined into a single dataset. Therefore, any subsequent analysis will be conducted on either site individually.

Table 7: Comparison of elemental concentrations in Middenbeemster vs Arnhem. (Table by Martijn Jacobs).

Element	Location	Mean	SD	P-value
Na	Middenbeemster	1.504	0.2749	0.0926
	Arnhem	1.603	0.2747	
Mg	Middenbeemster	**0.5543**	0.07280	**0.0034****
	Arnhem	0.5055	0.08228	
Al	Middenbeemster	**0.6721**	0.5006	**0.0005*****
	Arnhem	0.3333	0.2794	
Si	Middenbeemster	**2.845**	2.222	**<0.0001*****
	Arnhem	1.048	0.8928	
P	Middenbeemster	7.532	1.436	**<0.0001*****
	Arnhem	**9.362**	1.115	
S	Middenbeemster	**0.3107**	0.05081	**<0.0001*****
	Arnhem	0.2019	0.02775	
K	Middenbeemster	**0.2107**	0.1138	**<0.0001*****
	Arnhem	0.1316	0.04893	
Ca	Middenbeemster	19.86	2.242	**0.009*****
	Arnhem	**21.37**	1.830	
Ti	Middenbeemster	0.02977	0.0202	0.1314
	Arnhem	0.02063	0.01049	
Mn	Middenbeemster	0.1071	0.1103	0.1055
	Arnhem	0.1107	0.1764	
Fe	Middenbeemster	**0.5688**	0.3912	**0.0015****
	Arnhem	0.3674	0.2724	
Cu	Middenbeemster	0.006246	0.008805	0.1041
	Arnhem	0.00495	0.002383	
Zn	Middenbeemster	0.09892	0.06638	**0.0415***
	Arnhem	**0.1190**	0.0589	
As	Middenbeemster	**0.006385**	0.006661	**<0.0001*****
	Arnhem	0.002568	0.001556	
Sr	Middenbeemster	**0.02664**	0.007514	**<0.0001*****
	Arnhem	0.01946	0.004647	
Pb	Middenbeemster	**0.01697**	0.01971	**<0.0001*****
	Arnhem	0.007311	0.004430	

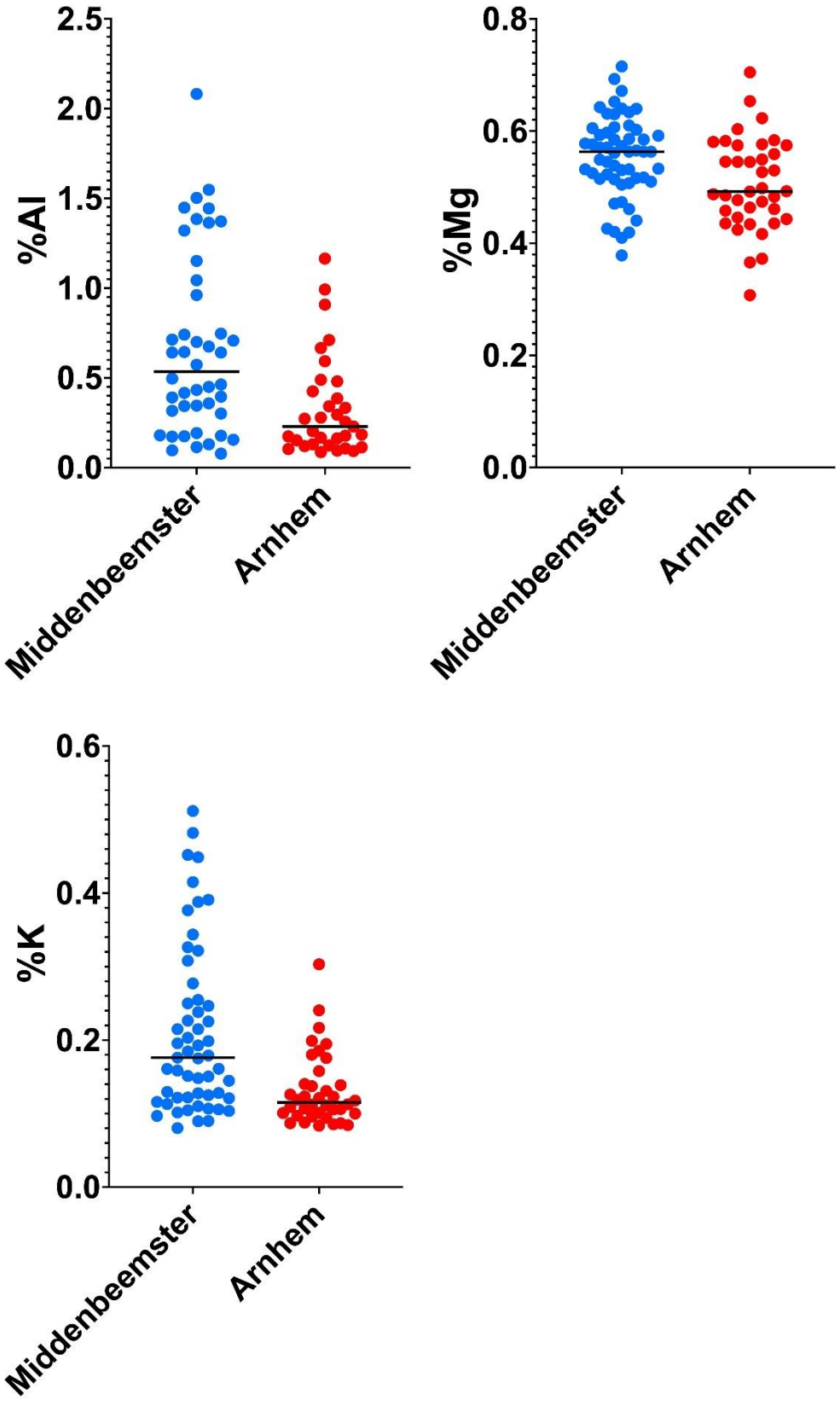

Figure 19: Scatter dot plots comparing concentrations in Al, Mg and K between Middenbeemster and Arnhem. (Figures by Martijn Jacobs).

After the comparison between Middenbeemster and Arnhem, a similar method was applied to compare the elemental concentrations of individuals from Middenbeemster with and without the presence of cribra femora (see table 8 & figure 20). Only one significant result was found, namely an increase in strontium in individuals with cribra femora.

Table 8: Comparison of elemental concentrations of individuals from Middenbeemster with and without cribra femora. (Table by Martijn Jacobs).

Element	Location	Mean	SD	P-value
Na	Cribra Femora	1.527	0.2770	0.2712
	No Cribra Femora	1.431	0.2648	
Mg	Cribra Femora	0.5541	0.7771	0.9731
	No Cribra Femora	0.5549	0.0567	
Al	Cribra Femora	0.6018	0.4395	0.0654
	No Cribra Femora	0.9456	0.6482	
Si	Cribra Femora	2.697	1.918	0.3783
	No Cribra Femora	3.325	3.052	
P	Cribra Femora	7.715	1.361	0.0898
	No Cribra Femora	6.941	1.570	
S	Cribra Femora	0.3137	0.05366	0.4355
	No Cribra Femora	0.3009	0.04054	
K	Cribra Femora	0.2032	0.09851	0.9127
	No Cribra Femora	0.2347	0.1559	
Ca	Cribra Femora	20.07	2.123	0.2133
	No Cribra Femora	19.18	2.562	
Ti	Cribra Femora	0.02913	0.02004	0.6279
	No Cribra Femora	0.03185	0.02835	
Mn	Cribra Femora	0.1086	0.1174	0.9491
	No Cribra Femora	0.08733	0.02835	
Fe	Cribra Femora	0.5818	0.4071	0.6201
	No Cribra Femora	0.5269	0.3467	
Cu	Cribra Femora	0.006572	0.009814	0.2385
	No Cribra Femora	0.005089	0.003530	
Zn	Cribra Femora	0.1005	0.06870	0.9172
	No Cribra Femora	0.09393	0.06057	
As	Cribra Femora	0.006576	0.007541	0.4471
	No Cribra Femora	0.005769	0.002187	
Sr	Cribra Femora	**0.02825**	0.007541	**0.0072****
	No Cribra Femora	0.02143	0.005842	
Pb	Cribra Femora	0.01755	0.02236	0.5468
	No Cribra Femora	0.01508	0.001621	

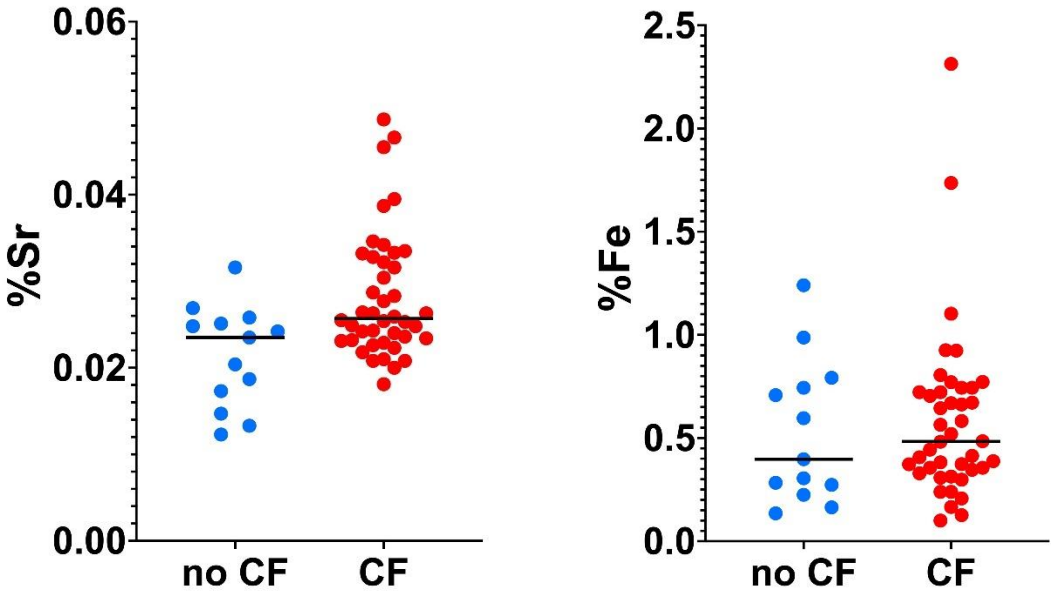

Figure 20: Scatter dot plots comparing concentrations in Sr and Fe between skeleton from Middenbeemster with and without cribra femora. (Figures by Martijn Jacobs).

The same comparison was then carried out for skeletons with and without cribra femora at Arnhem (see table 9 and figure 21). Here, the strontium values are not significantly different, but there are two other significant differences: individuals with cribra femora have higher concentrations of copper and zinc.

Table 9: Comparison of elemental concentrations in individuals from Arnhem with and without cribra femora. (Table by Martijn Jacobs).

Element	Location	Mean	SD	P-value
Na	Cribra Femora	1.555	0.3686	0.4145
	No Cribra Femora	1.631	0.2058	
Mg	Cribra Femora	0.4765	0.09382	0.0978
	No Cribra Femora	0.5224	0.07146	
Al	Cribra Femora	0.3252	0.3329	0.5009
	No Cribra Femora	0.3386	0.2477	
Si	Cribra Femora	1.072	1.141	0.4155
	No Cribra Femora	1.034	0.7463	
P	Cribra Femora	9.400	1.478	0.8748
	No Cribra Femora	9.340	0.8743	
S	Cribra Femora	0.1943	0.02501	0.1044
	No Cribra Femora	0.2063	0.02881	
K	Cribra Femora	0.1327	0.06189	0.5349
	No Cribra Femora	0.1309	0.04105	
Ca	Cribra Femora	21.36	2.185	0.9840
	No Cribra Femora	21.37	1.640	
Ti	Cribra Femora	0.02148	0.01091	0.7076
	No Cribra Femora	0.02013	0.01044	
Mn	Cribra Femora	0.1466	0.2487	0.5056
	No Cribra Femora	0.08980	0.1178	
Fe	Cribra Femora	0.3352	0.1921	0.7996

	No Cribra Femora	0.3861	0.3122	
Cu	Cribra Femora	**0.006254**	0.002249	**0.0114***
	No Cribra Femora	0.004213	0.002170	
Zn	Cribra Femora	**0.1414**	0.06164	**0.0337***
	No Cribra Femora	0.1059	0.05429	
As	Cribra Femora	0.002486	0.001335	0.999
	No Cribra Femora	0.002617	0.001697	
Sr	Cribra Femora	0.01976	0.004959	0.7629
	No Cribra Femora	0.01928	0.004555	
Pb	Cribra Femora	0.007114	0.003971	0.8347
	No Cribra Femora	0.007430	0.004771	

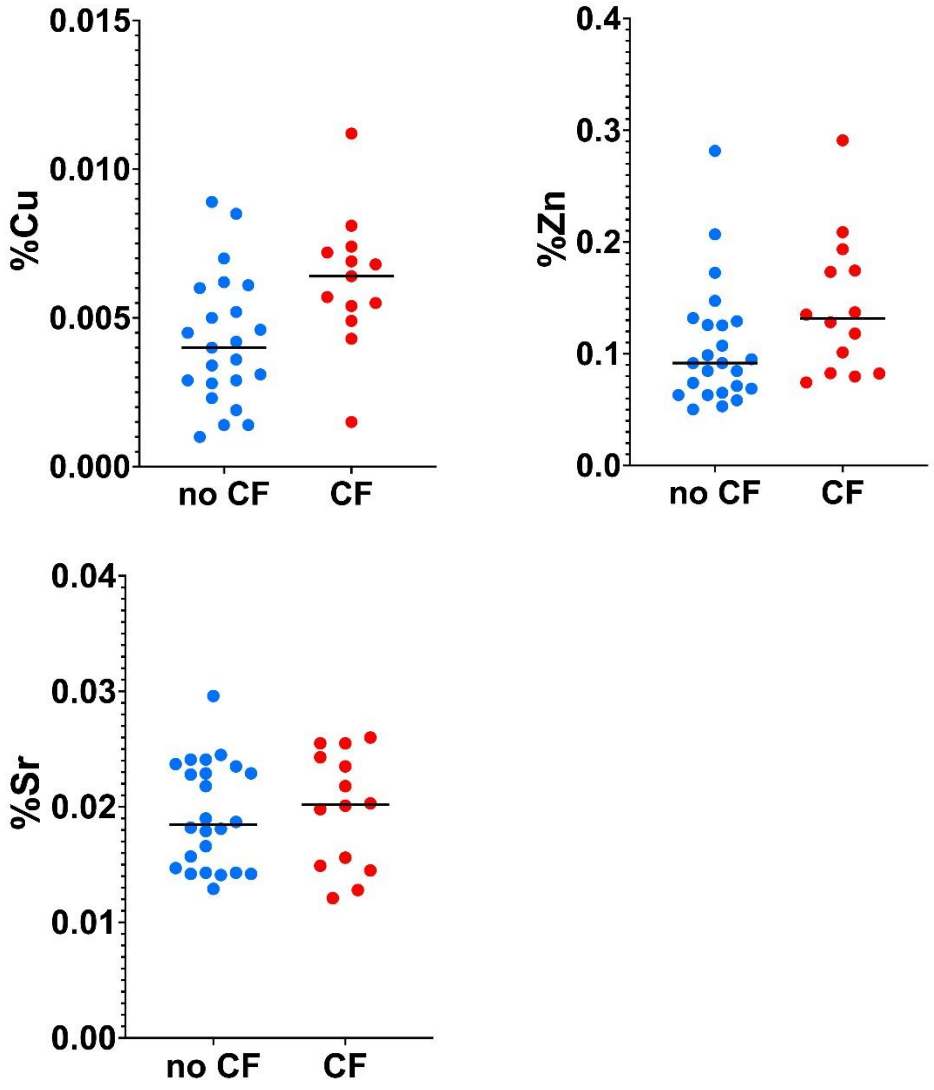

Figure 21: Scatter dot plots comparing concentrations in Ce, Zn, Sr between skeleton from Arnhem with and without cribra femora. (Figures by Martijn Jacobs).

In Middenbeemster, the only significant difference was found in strontium, with individuals with the condition having a higher concentration. At Arnhem, individuals with cribra femora had higher concentrations of copper and zinc in their femoral shaft.

Because we have previously asserted that cribra femora is much more frequent in the younger age-at-death categories, it is useful to compare the elemental concentrations in sub-adults and adults to see if there are any age-related differences that could affect the outcome of tables 8 and 9. The same method of comparison was applied here on skeletons from Middenbeemster (table 10 & figure 22). In total, four significant results were found: sub-adults at Middenbeemster have higher concentrations of potassium and strontium and lower concentrations of copper and zinc than adults from this site.

Table 10: Comparison of elemental concentrations between adults and sub-adutls from Middenbeemster. (Table by Martijn Jacobs).

Element	Location	Mean	SD	P-value
Na	Sub-adult	1.535	0.2828	0.2399
	Adult	1.441	0.2538	
Mg	Sub-adult	0.5564	0.07978	0.760
	Adult	0.5499	0.05767	
Al	Sub-adult	0.7163	0.5560	0.3165
	Adult	0.5397	0.2499	
Si	Sub-adult	3.252	2.476	0.0509
	Adult	2.010	1.265	
P	Sub-adult	7.629	1.542	0.4784
	Adult	7.333	1.206	
S	Sub-adult	0.3094	0.05254	0.5784
	Adult	0.3132	0.04843	
K	Sub-adult	**0.2316**	0.1271	**0.0495***
	Adult	0.1676	0.06343	
Ca	Sub-adult	20.06	2.447	0.3466
	Adult	19.45	1.738	
Ti	Sub-adult	0.03379	0.02479	0.051
	Adult	0.02149	0.01145	
Mn	Sub-adult	0.1201	0.1228	0.2868
	Adult	0.08041	0.07462	
Fe	Sub-adult	0.6211	0.4414	0.2338
	Adult	0.4612	0.006808	
Cu	Sub-adult	0.005736	0.009665	**0.0431***
	Adult	**0.007346**	0.006808	
Zn	Sub-adult	0.07882	0.05465	**0.0004*****
	Adult	**0.1403**	0.07059	
As	Sub-adult	0.006357	0.007553	0.3203
	Adult	0.006444	0.004486	
Sr	Sub-adult	**0.02829**	0.007466	**0.0396***
	Adult	0.02323	0.006563	
Pb	Sub-adult	0.01695	0.02248	0.3952
	Adult	0.01702	0.01280	

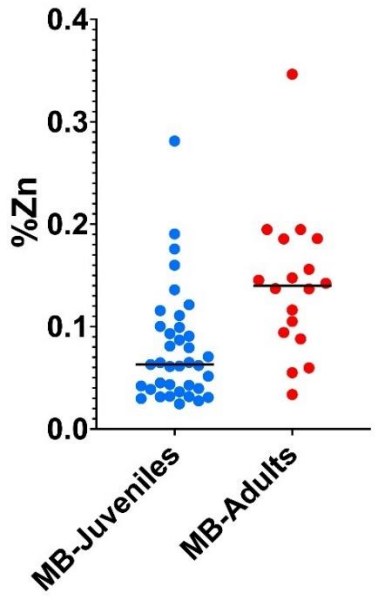

Figure 22: Scatter dot plot comparing concentrations of Zn between sub-adults and adults at Middenbeemster. (Figure by Martijn Jacobs).

Finally, the sub-adults and adults of Arnhem were compared (see table 11 & figure 23). This yielded only two significant results, namely that sub-adults at Arnhem have higher concentrations of both copper and zinc when compared to adults from this site.

Table 11: Comparison of elemental concentrations between adults and sub-adults from Arnhem. (Table by Martijn Jacobs).

Element	Location	Mean	SD	P-value
Na	Sub-adult	1.1613	0.3691	0.8714
	Adult	1.598	0.2194	
Mg	Sub-adult	0.5059	0.08875	0.9857
	Adult	0.5053	0.08062	
Al	Sub-adult	0.3494	0.3423	0.8974
	Adult	0.3241	0.2453	
Si	Sub-adult	1.153	1.198	0.5848
	Adult	0.9950	0.7192	
P	Sub-adult	9.398	1.517	0.8874
	Adult	9.343	0.8751	
S	Sub-adult	0.1927	0.02435	0.1086
	Adult	0.2066	0.02866	
K	Sub-adult	0.1367	0.06440	0.7559
	Adult	0.1289	0.03995	
Ca	Sub-adult	21.12	2.271	0.5538
	Adult	21.50	1.592	
Ti	Sub-adult	0.02384	0.01120	0.1391
	Adult	0.01896	0.00919	
Mn	Sub-adult	0.1860	0.2645	0.7020
	Adult	0.07160	0.09133	
Fe	Sub-adult	0.4290	0.2525	0.3214
	Adult	0.3353	0.2817	

Cu	Sub-adult	**0.006331**	0.002399	**0.0086**
	Adult	0.004170	0.002033	
Zn	Sub-adult	**0.1425**	0.06096	**0.0405**
	Adult	0.1067	0.05508	
As	Sub-adult	0.002723	0.002090	0.8494
	Adult	0.002488	0.001236	
Sr	Sub-adult	0.02132	0.004145	0.0743
	Adult	0.01849	0.004673	
Pb	Sub-adult	0.001150	0.004145	0.5039
	Adult	0.007454	0.004301.	

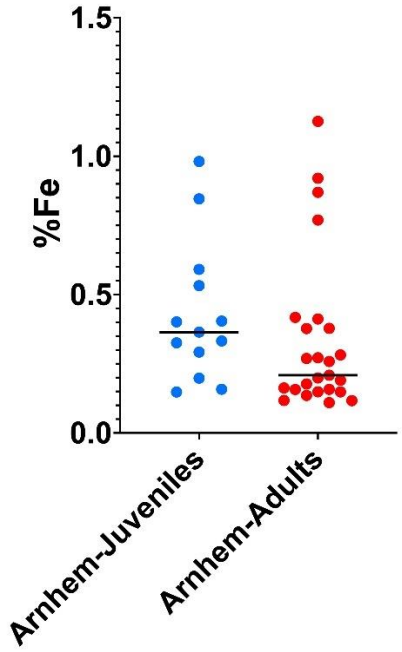

Figure 23: Scatter dot plot comparing concentration in Fe between sub-adults and adults from Arnhem. (Figure by Martijn Jacobs).

In the following chapter, these generated graphs and tables will be compared to each other. Based on this discussion, a number of conclusions will be drawn.

6: Discussion

In this chapter, we will discuss the generated results starting with the frequencies of porous lesions in regards to the different age-at-death groups and sexes. This is followed by a discussion on the elemental concentrations measured through pXRF and their meaning.

6.1 Frequency of porous lesions

The frequency graphs of cribra femora in both Middenbeemster and Arnhem show the anticipated downward trend, meaning that the lesions are most frequent in children and adolescents and that frequency goes down with increasing age-at-death. The Arnhem children only have a 50% frequency of cribra orbitalia, compared to 85% of children at Middenbeemster, but this most likely due to there only being a mere three children in the dataset, one of which had unobservable eye orbits. This downward trend matches with Stuart-Macadam's (1985) hypothesis that porous lesions are formed during childhood followed by a healing pattern. The same downward trend has also been observed in many other studies on this subject (Wapler et al., 2004; Walker et al., 2009; Schats, 2021; Gomes, 2022). As mentioned in the previous chapter, the adults of Middenbeemster were not sampled randomly but based on previous cribra femora diagnosis in their associated pathology reports with a number of controls added. This means that this section of the Middenbeemster cribra femora graph (see figure 14) has inflated frequencies. The Arnhem graph (see figure 15) is therefore a more accurate depiction of cribra femora across the different age groups.

Fisher's exact test was attempted to see if there were significant differences in the ratio of cribra femora vs no cribra femora in males and females. No significant difference in ratio could be found for Middenbeemster nor Arnhem. It should be noted that the sample size in this test is rather small due to sub-adults not having sex estimations, leaving only the adults.

The same test was then used for the ratio of cribra femora vs no cribra femora in adults and sub-adults. Because the Middenbeemster adult group was not sampled randomly, it could only be applied to the adults and sub-adults of Arnhem. Here, Fisher's exact test showed that the ratios were significantly different, with sub-adults having disproportionately many cases of the condition. The reciprocal odds ratio for Arnhem is 40.33, meaning that the chance of a sub-adult being diagnosed with cribra femora is 40 times higher than an adult from the same site. This further supports the above mentioned theory of Stuart-Macadam (1985) that porous lesions are formed during childhood and in most individuals heal into adulthood.

6.2 pXRF measurements of elemental concentrations

As we compare the elemental concentrations between the sites of Middenbeemster and Arnhem, we can see that for most elements, the concentrations have statistically significant differences. This is an important observation because it demonstrates that the variation between sites is larger than their internal variability. When using pXRF to study skeletal remains, one should therefore not combine the measured elemental concentrations of different excavations into a larger dataset. When an excavation site is heterogeneous in nature, for example containing multiple burial grounds from vastly different eras or site locations, it should be recommended to check for differences in elemental concentrations between these groups. By comparing the concentrations of different sites as well as in vivo concentrations, we can possibly identify concentrations that have been severely altered through diagenesis. For example, in their pXRF study of skeletons from Coach Lane, Kilburn et al. (2021, p. 5) found that the detected levels of aluminium and titanium were much higher than the expected in vivo

levels. This was deemed to most likely the result of industrial activities in the vicinity of the burial ground.

For example, heavy industry has also caused widespread contamination in the Netherlands. The zinc factory Budel in Noord-Brabant has contaminated most of the South-Eastern Netherlands with high levels of zinc, including large parts of the provinces of Noord-Brabant, Gelderland and Limburg (Edelman, 1982).

The concept of diagenesis remains problematic within the portable X-ray fluorescence, especially in a material as porous as human bone remains. First there is the question of whether a significant difference in elemental concentration represents a different concentration in vivo, or if it resulted from the leaking and/or absorption of certain elements after burial.

To illustrate this, take the site of Middenbeemster which has a significantly higher concentration of iron compared to Arnhem, but also significantly higher concentrations of arsenic and lead. Arsenic was common in the 18th and 19th centuries, this toxic element was used in a wide variety of medicines treating conditions such as fevers, malaria, syphilis among others (Gibeaud & Jaouen, 2010). It was also used in other items such as make-up and pigments. Lead was also very common in the past taking many forms like tableware of water pipes (Rabin, 2008). Both arsenic and lead are also frequent contaminants in soil today: arsenic compounds are used in a range of insecticides and herbicides, as well as treating wood (Rahman et al. 2004). Lead contamination can result from a wide range of sources such as industrial processes, but one of the most important is tetraethyllead, which was used in motor fuel from the 1920's until quite recently, causing worldwide lead pollution (Kovarik, 2005). To complicate matters even further, arsenic was also frequently used in the embalming process during the 19th and early 20th century United States (Meyers et al., 2020).

This means that increased concentrations of this specific element in a skeleton can be either caused by arsenic intake during the life of the individual, post-mortem during the embalming process, after death through diagenesis or any combination of these factors. In the case of Middenbeemster embalming seems to be an unlikely factor as this was mainly popular in the USA, but it can not be determined with absolute certainty whether arsenic intake or diagenetic processes are responsible.

Another aspect within diagenesis that should be taken into account is the fact that not all elements are created equal when it comes to usefulness in a biological context. A large number of organisms like fungi, bacteria and microorganisms in the soil are involved in the process. Therefore biologically important elements like calcium, phosphor or iron are more likely to be consumed than elements with lesser biological importance such as titanium. This differential organism absorption could distort the relative concentrations within a sample.

The main problem in pXRF of human skeletal remains boils down to the fact that it can only measure the outer cortex of the bone with very little penetration power. Clarke (2008, p. 131) shows that sanding down the measurement area prior to the pXRf-analysis can help with this, but this would beat the main advantage of the technique, namely its non-destructiveness. If a destructive technique is used, one can better choose a technique that generates a higher accuracy, like LA-ICP-MS.

The best way to counter the abovementioned problems seems to take soil samples from the excavation site, preferably from each individual burial as there may be significant differences within the site. For Middenbeemster and Arnhem these were unfortunately not available. It was considered in this study to scrape off some sediment that is stuck to some of the Middenbeemster skeletons that have not yet been washed, but this was ultimately decided against because it cannot be asserted to

what degree is chemical composition has changed over centuries of direct contact with the cortical bone. After all, it is better not to use a soil sample than a wrong soil sample.

A possible way forward may be the application of experimental archaeology, whereby the elemental composition of some animal bones would be measured through portable X-ray fluorescence, before being buried for a set amount of time. When the bones are excavated again they could be analysed through pXRF a second time with the results being compared to the original composition. While this could definitely help improve our understanding of pXRF-analysis on human bones, even this can not control for all variables such as soil acidity at the burial site which will lead to stronger degradation of the bone.

When researching possible correlations between elemental concentrations in skeletal remains and certain pathological conditions, if possible, one should try to incorporate other archaeometric techniques to counter the uncertainty that is inherent in elemental compositions of bone. For example, Zdral et al. (2021) make use of Dual-Energy X-ray Absorptiometry (DXA) to measure the bone density of femora and compare this with the pXRF-measurements to investigate osteoporosity.

6.3 Elemental concentration analysis

In the current study, we have compared the elemental composition of individuals with and without cirbra femora for both the Middenbeemster and Arnhem sites. It was hypothesized that if the condition indeed results from red marrow hyperplasia due to iron-deficiency anaemia, a significantly lower iron concentration would be detected in the individuals with cribra femora. However, for both the Middenbeemster and Arnhem sites, no significant difference in iron concentration was found between individuals with and without cribra femora.

In fact, for Middenbeemster the only significant difference between both groups was found in concentration of strontium. This element has chemical properties that are similar to those of calcium and is easily stored in human bones. It mainly enters the body through the consumption of grains, leafy greens and water, although only 25-30% of the consumed strontium is absorbed (Kolodziejska et al., pp. 1-2). Because cribra femora is much more frequent in sub-adults than adults, these two groups were also compared for elemental concentrations in order to check for disparities due to bone development. The same significant difference with a higher strontium concentration was found in the Middenbeemster sub-adults compared to adults. This seems to indicate that the higher strontium level in individuals with cribra femora is likely due to this group being mostly comprised out of sub-adults. Possibly the higher concentration is caused the high rate of bone growth causing more strontium to absorbed.

In the comparison of individuals with and without cribra femora at Arnhem, just two significant differences were found in their elemental concentrations. In individuals without cribra femora, the concentrations of both copper and zinc is lower than those that have cribra femora. However, just like the strontium level at Middenbeemster, the copper and zinc concentrations at Arnhem also show the same significant differences when comparing sub-adults with adults. In the case of Arnhem, cribra femora is so frequent in sub-adults that it is difficult to compare both groups.

Zinc plays an important role in erythropoiesis and deficiency of it can lead to anaemia. Interestingly, zinc can also cause anaemia when it is present in excess (Jeng & Cheng, 2022). When too much zinc is present in the body, this can inhibit copper being taken up in the blood plasma, resulting in copper deficiency anaemia (Myint et al., 2018). Several clinical examples have been recorded where individuals with and excessive zinc intake, usually due to zinc supplements, develop copper deficiency

anaemia which is sometimes misdiagnosed as iron deficiency anaemia (Hoogenraad et al., 1985; Hoffman et al., 1988; Botash et al., 1992).

Copper deficiency anaemia will affect marrow haematopoiesis as well as certain neurological functions (Cordano, 1998). In the case Arnhem however, the copper concentration is actually higher in individuals with cribra femora/sub-adults, while one would expect a lower concentration in the case of zinc-induced copper deficiency anaemia. It is therefore likely that the significantly higher concentration of copper in sub-adults is due to higher copper absorption and retention rates in sub-adults compared to adults, although diagenetic processes can of course not be excluded. Unfortunately, nearly all research on copper absorption has focused on either infants or adults, with no clear data available for the absorption rates in children and adolescents (Lönnerdal, 1998, p. 1048). Yet, it has been shown that infants have a higher absorption rate of copper compared to adults, with healthy adults having and absorption rate of 12 – 71% and infants 75 – 84% (US Department of Health and Human Services, 2022). It therefore seems likely that the higher concentration of copper is the result of higher absorption in children and adults and not related to cribra femora.

In Middenbeemster, significant differences for copper and zinc were also found when comparing sub-adults with adults. While zinc levels are higher in sub-adults, copper levels are actually lower. Yet when comparing Middenbeemster individuals with and without cribra femora, no significant differences were found for either copper or zinc. So even if this could possible indicate zinc-induced copper deficiency, it cannot be connected to cribra femora. There is also an important caveat, namely that hundreds of coffin fittings were found at Middenbeemster which are often made out of zinc or zinc-alloys (Hakvoort, 2013, p. 71). This possible source of contamination means that any conclusions regarding zinc on this site should be carefully considered. Further studies adults and sub-adults from different sites will be useful to compare with the date from Arnhem and Middenbeemster.

In conclusion, the data generated by pXRF show that individuals with cribra femora do not have significantly different iron levels than those without the condition. Iron-deficiency is therefore most-likely not the underlying cause in the majority of cribra femora cases. Significant differences in strontium, copper or zinc are probably due to developmental factors and not related to cribra femora, so (zinc-induced) copper deficiency anaemia are also unlikely to form the aetiology. These results do not mean that cribra femora cannot result from anaemia. As discussed before, there are a wide range of anaemia types, for example megaloblastic anaemia which is caused by a deficiency in vitamin B12. This study only shows that the specific type of anaemia, iron deficiency anaemia, is most likely not the underlying cause in most case of cribra femora at Middenbeemster and Arnhem. It should be considered a warning to archaeologists, similar to that of Wapler et al. (2004), that one cannot simply interpret porous skeletal lesions as evidence of (iron-deficiency- anaemia.

7: Conclusions

In this study, we have considered the various practical implications of applying portable X-ray fluorescence in human osteoarchaeology. Although pXRF has become quite common in geology and archaeometry, the application of this technique is still in its infancy for osteoarchaeology. After considering protocols by other researchers, it was determined that the best method for pXRF measurement of human skeletal remains were to take top-down measurements with pXRF mounted horizontally to a tripod. Every measurement was taken on the same type of bone at the same location, in order to avoid intra-skeletal variations due to differences in cortical thickness.

Besides the measurements of elemental compositions, macroscopic observations were used to identify cribra femora and cribra orbitalia on the femoral neck and eye orbits respectively. The acquired frequency confirmed the sub-hypothesis that the both porous lesions under study are more frequent in sub-adults than adults and show a downward trend with increasing age-at-death. No significant differences in the ratio of cribra femora could be found between males and females.

The comparison in elemental compositions showed no significant differences in iron concentrations for either Middenbeemster of Arnhem, which likely indicates that iron deficiency anaemia is not an underlaying cause in the majority of cribra femora cases at these sites. A few significant differences were found for the elements strontium, copper and zinc, but these were shown to most likely be due to developmental factors and unrelated to cribra femora.

It should be stated that the findings do not exclude all types of anaemia as possible causes for cribra femora, only the specific type resulting from iron deficiency. Other types of anaemia with different causes such as vitamin B12 deficiency could potentially still result in cribra femora. Most important is that it should be clear that one cannot simply equate the presence of cribra femora with iron deficiency. In archaeology, cribra femora has been used as a proxy for studying iron intake and other nutritional information in past populations, but this paper indicates that this assumption is unfounded.

Because of its little penetration power, pXRF-analysis of human bone can be quite vulnerable to diagenetic processes. Potentially, the use frequent on-site soil sampling could help alleviate this problem to some extent. If possible, the combination of other archaeometric techniques with pXRF would make it more suitable for the study of human remains. It was also considered that future experimental research could possibly increase our understanding of chemical absorption and/or leaking of bone material, especially the outer cortex.

The current study has demonstrated some of the main advantages of applying pXRF-analysis in human osteoarchaeology. The most important of which is that no additional costs were made for the analyses. Combined with the speed and non-invasiveness of the technique compared to traditional analysis techniques. It is therefore likely that pXRF-use in human osteoarchaeology will see significant growth in the coming years.

pXRF-analysis was able to distinguish skeletons buried at Arnhem from those at Middenbeemster. Although not the focus of this paper, it demonstrates the techniques potential for differentiating between burial locations. This could possibly be used to differentiate skeletons that were reburied from different burial locations after their original graves where cleared. However, much more research on this topic needs to be done before it can be determined if this is an actual possibility.

For future research, it would be useful if the study was repeated on a modern osteological collection where basic medical background information is available for (part of) the skeletons under study. This

approach would have a smaller error margin because features such as sex of age-at-death are recorded and do not need to be estimated.

The majority of research on this subject still originates from osteoarchaeology. While there are some clinical studies of patients with porous lesions in vivo, these are few and far apart. More attention from medical sciences could probably increase our understanding of the topic significantly.

It is also recommended for any other future studies of porous lesions not to limit themselves to purely macroscopic techniques, but also incorporate at least one chemical analysis in their study. For this, portable X-ray fluorescence has been shown to be an efficient method, because of its low operating costs, fast measurements, high mobility and complete non-invasiveness towards the sample in question.

Abstract

Porous lesion of the eye orbits, cranial vault, femoral neck and proximal humerus are called porous lesions. Traditionally the first two, cribra orbitalia and cribra cranii, have been considered to originate from iron deficiency anaemia. As such, they have been used as a proxy for studying iron deficiency and anaemia in ancient populations, even though there is still no consensus on their aetiology.

In this study, we apply the technique of portable X-ray Fluorescence Spectrometry to skeletons from the archaeological sites of Middenbeemster and Arnhem in order to measure the elemental concentrations of the bone in a non-invasive way. For both sites, no significant differences in iron concentrations were found between individuals with and without cribra femora. This seems to indicate that iron deficiency anaemia is not the underlying cause of cribra femora.

Bibliography

Angel, J. L. (1966). Porotic hyperostosis, anemias, malarias, and marshes in the prehistoric Eastern Mediterranean. *Science (New York, N.Y.)*, *153*(3737), 760–763. https://doi.org/10.1126/science.153.3737.760

Bezur, A., Lee, L., Loubser, M., & Trentelman, K. (2020). *Handheld XRF in cultural heritage: A practical workbook for conservators*. The Getty Conservation Institute.

Botash, A. S., Nasca, J., Dubowy, R., Weinberger, H. L., & Oliphant, M. (1992). Zinc-induced copper deficiency in an infant. *American Journal of Diseases of Children (1960)*, *146*(6), 709–711. https://doi.org/10.1001/archpedi.1992.02160180069019

Brandow, A. M., & Liem, R. I. (2022). Advances in the diagnosis and treatment of sickle cell disease. *Journal of Hematology & Oncology*, *15*(1), 20. https://doi.org/10.1186/s13045-022-01237-z

Brickley, M. B. (2018). Cribra orbitalia and porotic hyperostosis: A biological approach to diagnosis. *American Journal of Physical Anthropology*, *167*(4), 896–902. https://doi.org/10.1002/ajpa.23701

Brickley, M. B., Ives, R., & Mays, S. (Eds.). (2020). Anaemia. In *The Bioarchaeology of Metabolic Bone Disease (Second Edition)*. Academic Press. https://doi.org/10.1016/B978-0-08-101020-4.00012-4

Brooks, S., & Suchey, J. M. (1990). Skeletal age determination based on the os pubis: A comparison of the Acsádi-Nemeskéri and Suchey-Brooks methods. *Human Evolution*, *5*(3), 227–238. https://doi.org/10.1007/BF02437238

Buckberry, J. L., & Chamberlain, A. T. (2002). Age estimation from the auricular surface of the ilium: A revised method. *American Journal of Physical Anthropology*, *119*(3), 231–239. https://doi.org/10.1002/ajpa.10130

Buikstra, J., & Ubelaker, D. (1994). *Standards for data collection from human skeletal remains*. Arkansas Archaeological Survey.

Byrnes, J. F., & Bush, P. J. (2016). Practical Considerations in Trace Element Analysis of Bone by Portable X-ray Fluorescence. *Journal of Forensic Sciences*, *61*(4), 1041–1045. https://doi.org/10.1111/1556-4029.13103

Carlson, D., Armelagos, G., & Van Gerven, D. (1974). Factors influencing the etiology of cribra orbitalia in prehistoric Nubia. *Journal of Human Evolution*, *3*, 405-410.

Chakravorty, S., & Williams, T. N. (2015). Sickle cell disease: A neglected chronic disease of increasing global health importance. *Archives of Disease in Childhood*, *100*(1), 48–53. https://doi.org/10.1136/archdischild-2013-303773

Clarke, B. (2008). Normal Bone Anatomy and Physiology. *Clinical Journal of the American Society of Nephrology : CJASN*, *3*(Suppl 3), S131–S139. https://doi.org/10.2215/CJN.04151206

Cordano, A. (1998). Clinical manifestations of nutritional copper deficiency in infants and children. *The American Journal of Clinical Nutrition*, *67*(5), 1012S-1016S. https://doi.org/10.1093/ajcn/67.5.1012S

Eusebius Arnhem. *Over de Eusebius*. (n.d.). Retrieved 27 April 2023, from https://eusebius.nl/over-de-eusebius/

Edelman, Theo. (1982). Zware metalen van zinkfrabiek belasten het milieu tot op 25km. [Unknown Journal]. 10-13.

Ferembach, D., Schwindezky, I., & Stoukal, M. (1980). Recommendation for Age and Sex Diagnoses of Skeletons. *Journal of Human Evolution*, *9*, 517–549.

Forster, N., Grave, P., Vickery, N., & Kealhofer, L. (2011). Non-destructive analysis using PXRF: Methodology and application to archaeological ceramics. *X-Ray Spectrometry*, *40*(5), 389–398. https://doi.org/10.1002/xrs.1360

Galea, J. (2013). *Analysing the miocroarchitecture of cribra orbitalia via micro-computed tomography in post-medieval remains from the Bristol Royal Infirmary*. [Master's Thesis, University of Bristol]. https://doi.org/10.13140/2.1.1243.6803

Gibaud, S., & Jaouen, G. (2010). Arsenic-Based Drugs: From Fowler's Solution to Modern Anticancer Chemotherapy. In G. Jaouen & N. Metzler-Nolte (Eds.), *Medicinal Organometallic Chemistry* (pp. 1–20). Springer. https://doi.org/10.1007/978-3-642-13185-1_1

Göhring, A. (2021). Allen's fossa - An attempt to dissolve the confusion of different nonmetric variants on the anterior femoral neck. *International Journal of Osteoarchaeology*, *31*(4), 513–522. https://doi.org/10.1002/oa.2968

Gomes, R., Catarino, L., & Santos, A. L. (2021). Anemia, cribra cranii and elemental composition using portable X-ray fluorescence: A study in individuals from the Coimbra Identified Osteological Collections. *Journal of Archaeological Science*, *136*, 105514. https://doi.org/10.1016/j.jas.2021.105514

Gomes, R., Petit, J., Dutour, O., & Santos, A. L. (2022). Frequency and co-occurrence of porous skeletal lesions in identified non-adults from Portugal (19th to 20th centuries) and its association with respiratory infections as cause of death. *International Journal of Osteoarchaeology*, *32*(5), 1061–1072. https://doi.org/10.1002/oa.3132

Hakvoort, A. (2013). De begravingen bij de Keyserkerk te Middenbeemster. *Hollandia*, *464*, 1-149.

Henderson, J. (2019). Measuring Trace Element Concentrations in Artiodactyl Cannonbones using Portable X-Ray Fluorescence. [Unpublished Master's Thesis, Central Washington University]. https://digitalcommons.cwu.edu/etd/1128

Hoffman, H. N., Phyliky, R. L., & Fleming, C. R. (1988). Zinc-induced copper deficiency. *Gastroenterology*, *94*(2), 508–512. https://doi.org/10.1016/0016-5085(88)90445-3

Hoogenraad, T. U., Dekker, A. W., & van den Hamer, C. J. (1985). Copper responsive anemia, induced by oral zinc therapy in a patient with acrodermatitis enteropathica. *The Science of the Total Environment*, *42*(1–2), 37–43. https://doi.org/10.1016/0048-9697(85)90005-1

Işcan, M. Y., Loth, S. R., & Wright, R. K. (1985). Age estimation from the rib by phase analysis: White females. *Journal of Forensic Sciences*, *30*(3), 853–863.

Jeng, S., & Chen, Y.-H. (2022). Association of Zinc with Anemia. *Nutrients*, *14*(22), 4918. https://doi.org/10.3390/nu14224918

Kilburn, N., Gowland, R. L., Halldórsdóttir, H., Williams, R., & Thompson, T. (2021). Assessing pathological conditions in archaeological bone using portable X-ray fluorescence (pXRF). *Journal of Archaeological Science: Reports*, *37*(102980). https://doi.org/10.1016/j.jasrep.2021.102980

Kricun, M. E. (1985). Red-yellow marrow conversion: Its effect on the location of some solitary bone lesions. *Skeletal Radiology*, *14*(1), 10–19. https://doi.org/10.1007/BF00361188

Kołodziejska, B., Stępień, N., & Kolmas, J. (2021). The Influence of Strontium on Bone Tissue Metabolism and Its Application in Osteoporosis Treatment. *International Journal of Molecular Sciences*, *22*(12), 6564. https://doi.org/10.3390/ijms22126564

Kovarik, W. (2005). Ethyl-leaded gasoline: How a classic occupational disease became an international public health disaster. *International Journal of Occupational and Environmental Health*, *11*(4), 384–397. https://doi.org/10.1179/oeh.2005.11.4.384

Lemmers, S., Schats, R., Hoogland, M., & Waters-Rist, A. (2013). Fysisch anthropologische analyse middenbeemster. *Hollandia*, *464*, 35–60.

Lönnerdal, B. (1998). Copper nutrition during infancy and childhood. *The American Journal of Clinical Nutrition*, *67*(5 Suppl), 1046S-1053S. https://doi.org/10.1093/ajcn/67.5.1046S

Maat, G. (2001). Diet and age-at-death determinations from molar attrition. A review related to the low countries. *The Journal of Forensic Odonto-Stomatology*, *19*, 18–21.

Mangas-Carrasco, E., & López-Costas, O. (2021). Porotic hyperostosis, cribra orbitalia, femoralis and humeralis in Medieval NW Spain. *Archaeological and Anthropological Sciences*, *13*(10). https://urn.kb.se/resolve?urn=urn:nbn:se:su:diva-198524

Małkiewicz, A., & Dziedzic, M. (2012). Bone marrow reconversion – imaging of physiological changes in bone marrow. *Polish Journal of Radiology*, *77*(4), 45–50.

McGarry, A., Floyd, B., & Littleton, J. (2021). Using portable X-ray fluorescence (pXRF) spectrometry to discriminate burned skeletal fragments. *Archaeological and Anthropological Sciences*, *13*(7), 117. https://doi.org/10.1007/s12520-021-01368-3

Meindl, R. S., & Lovejoy, C. O. (1985). Ectocranial suture closure: A revised method for the determination of skeletal age at death based on the lateral-anterior sutures. *American Journal of Physical Anthropology*, *68*(1), 57–66. https://doi.org/10.1002/ajpa.1330680106

Meyers, M. S., Breetzke, D., & Holt, H. (2021). Arsenic and Old Graves: A Method for Testing Arsenic Contamination in Historic Cemeteries. *Advances in Archaeological Practice*, *9*(1), 34–40. https://doi.org/10.1017/aap.2020.41

Miquel-Feucht, M., Polo-Cerda, M., & Villalaín-Blanco, M. (1999). El síndrome criboso: criba femoral vs criba orbitaria. In Sanchez, J.A. (Ed.), *Sistematizacion Methodologica En Paleopathlogía*, Actas V Congreso Nacional AEP. Asociacíon Espanola de Paleopathología.

Muncie, H. L., & Campbell, J. (2009). Alpha and beta thalassemia. *American Family Physician*, *80*(4), 339–344.

Muskara, U., & Kalaycı, K. (2021). The feasibility of pXRF for discrimination attic black-figure painters using pigment analysis. *Mediterranean Archaeology and Archaeometry*, *21*, 237–255. https://doi.org/10.5281/zenodo.4574639

Myint, Z. W., Oo, T. H., Thein, K. Z., Tun, A. M., & Saeed, H. (2018). Copper deficiency anemia: Review article. *Annals of Hematology*, *97*(9), 1527–1534. https://doi.org/10.1007/s00277-018-3407-5

Obertova, Z., & Thurzo, M. (2004). Cribra orbitalia as an Indicator of Stress in the Early Medieval Slavic Population from Borovce (Slovakia). *Anthropologie 42*(2), 189-194.

O'Brien, A., & McDonald, S. W. (2007). The meningo-orbital foramen in a Scottish population. *Clinical Anatomy*, *20*(8), 880–885. https://doi.org/10.1002/ca.20558

O'Donnell, L., Hill, E. C., Anderson, A. S. A., & Edgar, H. J. H. (2020). Cribra orbitalia and porotic hyperostosis are associated with respiratory infections in a contemporary mortality sample from New Mexico. *American Journal of Physical Anthropology*, *173*(4), 721–733. https://doi.org/10.1002/ajpa.24131

Oxenham, M. F., & Cavill, I. (2010). Porotic hyperostosis and cribra orbitalia: The erythropoietic response to iron-deficiency anaemia. *Anthropological Science*, *118*(3), 199–200. https://doi.org/10.1537/ase.100302

Penn Medicine. (n.d.). *Anemia—Symptoms and Causes*. Retrieved 9 May 2023, from https://www.pennmedicine.org/for-patients-and-visitors/patient-information/conditions-treated-a-to-z/anemia

Perrone, A., Finlayson, J., Bartelink, E., & Dalton, K. (2014). Application of Portable X-ray Fluorescence (XRF) for Sorting Commingled Human Remains . In Adams, B., & Byrd, J. *Commingled Human Remains: Methods in Recovery, Analysis, and Identification* (pp. 145–165). Academic Press. https://doi.org/10.1016/B978-0-12-405889-7.00007-1

RAAP bv. (2017). Van ondergrondse naar bovengronds beek. *RAAP magazine*, *2*, 1. https://www.raap.nl/magazine/RAAPMAGAZINE201702/index.html#extFeatures9-2

Rahman, F. A., Allan, D. L., Rosen, C. J., & Sadowsky, M. J. (2004). Arsenic Availability from Chromated Copper Arsenate (CCA)–Treated Wood. *Journal of Environmental Quality*, *33*(1), 173–180. https://doi.org/10.2134/jeq2004.1730

Rabin, R. (2008). The Lead Industry and Lead Water Pipes "A MODEST CAMPAIGN". *American Journal of Public Health*, *98*(9), 1584–1592. https://doi.org/10.2105/AJPH.2007.113555

Rivera, F., & Mirazón Lahr, M. (2017). New evidence suggesting a dissociated etiology for cribra orbitalia and porotic hyperostosis. *American Journal of Physical Anthropology*, *164*(1), 76–96. https://doi.org/10.1002/ajpa.23258

Schats, R. (2021). Cribriotic lesions in archaeological human skeletal remains. Prevalence, co-occurrence, and association in medieval and early modern Netherlands. *International Journal of Paleopathology*, *35*, 81–89. https://doi.org/10.1016/j.ijpp.2021.10.003

Sealey, I., Morgan, B., Ribot, I., & Brickley, M. (2022, October 26-29). *Can cribra femora be utilized to evaluate anemia in non-adults: An investigation using micro-CT analysis*. CABA-ACAB 49th Annual Meeting, Sashkatoon, Canada.

Serjeant, G. R. (2010). One hundred years of sickle cell disease. *British Journal of Haematology*, *151*(5), 425–429. https://doi.org/10.1111/j.1365-2141.2010.08419.x

Shoval, S., & Gilboa, A. (2016). PXRF analysis of pigments in decorations on ceramics in the East Mediterranean: A test-case on Cypro-Geometric and Cypro-Archaic Bichrome ceramics at Tel Dor, Israel. *Journal of Archaeological Science: Reports*, *7*, 472–479. https://doi.org/10.1016/j.jasrep.2015.08.011

Srikanth, S. (2016). Megaloblastic anemia - A clinical spectrum and a hematological profile: The day-to-day public health problem. *Medical Journal of Dr. D.Y. Patil University*, *9*(3), 307-310. https://doi.org/10.4103/0975-2870.182497

Stuart-Macadam, P. (1985). Porotic hyperostosis: Representative of a childhood condition. *American Journal of Physical Anthropology*, *66*(4), 391–398. https://doi.org/10.1002/ajpa.1330660407

Tykot, R. H. (2016). Using Nondestructive Portable X-ray Fluorescence Spectrometers on Stone, Ceramics, Metals, and Other Materials in Museums: Advantages and Limitations. *Applied Spectroscopy*, *70*(1), 42–56. https://doi.org/10.1177/0003702815616745

US Department of Health and Human Services. (2022). *Toxicological Profile for Copper*. https://www.atsdr.cdc.gov/toxprofiles/tp132.pdf

Van Nuland, M. (2019, June 14). *Een kleine ode aan 412 doden*. Universiteit Leiden. https://www.universiteitleiden.nl/nieuws/2019/06/een-kleine-ode-aan-412-doden

Vyas, K. K., Patel, V. P., Joshi, A., & Shroff, B. D. (2013). An osseous study of non-metric variation of the neck of the femur. *International Journal of Research in Medical Sciences*, *2*(1), 98-100.

Volstellingen. (2022). *Volkstellingen 1795-1971*. http://www.volkstellingen.nl/

Walker, P. L., Bathurst, R. R., Richman, R., Gjerdrum, T., & Andrushko, V. A. (2009). The causes of porotic hyperostosis and cribra orbitalia: A reappraisal of the iron-deficiency-anemia hypothesis. *American Journal of Physical Anthropology*, *139*(2), 109–125. https://doi.org/10.1002/ajpa.21031

Wambua, S., Mwangi, T. W., Kortok, M., Uyoga, S. M., Macharia, A. W., Mwacharo, J. K., Weatherall, D. J., Snow, R. W., Marsh, K., & Williams, T. N. (2006). The Effect of α +-Thalassaemia on the Incidence of Malaria and Other Diseases in Children Living on the Coast of Kenya. *PLoS Medicine*, *3*(5), e158. https://doi.org/10.1371/journal.pmed.0030158

Wapler, U., Crubézy, E., & Schultz, M. (2004). Is cribra orbitalia synonymous with anemia? Analysis and interpretation of cranial pathology in Sudan. *American Journal of Physical Anthropology*, *123*(4), 333–339. https://doi.org/10.1002/ajpa.10321

Williams, R., Taylor, G., & Orr, C. (2020). PXRF method development for elemental analysis of archaeological soil. *Archaeometry*, *62*(6), 1145–1163. https://doi.org/10.1111/arcm.12583

Zdilla, M. J., Nestor, N. S., Rothschild, B. M., & Lambert, H. W. (2022). Cribra orbitalia is correlated with the meningo-orbital foramen and is vascular and developmental in nature. *The Anatomical Record*, *305*(7), 1629–1671. https://doi.org/10.1002/ar.24825

Zdral, S., Monge Calleja, Á. M., Catarino, L., Curate, F., & Santos, A. L. (2021). Elemental Composition in Female Dry Femora Using Portable X-Ray Fluorescence (pXRF): Association with Age and Osteoporosis. *Calcified Tissue International*, *109*(2), 231–240. https://doi.org/10.1007/s00223-021-00840-5.

Appendix

Site	Feature number	Find number	Cribra femora	Cribra orbitalia	Estimated age	Sex	Na	Mg	Al	Si	P	S	K	Ca	Ti	Mn	Fe	Cu	Zn	As	Sr	Pb
Midden-Beemster	S47	V45	yes	No	YA	Female	1,8039	0,5732	0,3429	2,9059	4,9861	0,243	0,2547	17,6531	0,046	0,0269	0,3823	0,0016	0,1559	0,0045	0,0208	0,0112
Midden-Beemster	S060	V0037	yes	No	YA	Female	1,5753	0,5072	< LOD	0,4058	9,6093	0,2331	0,09	21,9066	0,008	0,0067	0,0999	0,0023	0,1369	0,0054	0,0328	0,0169
Midden-Beemster	S260	v1503	yes	NA	YA	Probable male	1,281	0,5707	0,1925	1,3337	8,6676	0,3759	0,125	21,1767	0,0155	0,0501	0,3291	< LOD	0,105	0,0034	0,0287	0,0099
Midden-Beemster	S289	V477	yes	No	OA	Male	0,9761	0,5848	0,573	3,8934	5,0615	0,2853	0,2465	15,9324	0,0385	0,2154	0,6626	< LOD	0,1476	0,0077	0,0333	0,0202
Midden-Beemster	S310	V550	yes	Yes	YA	Male	1,4626	0,5316	< LOD	0,6826	7,0747	0,3865	0,1586	19,025	0,0139	0,0143	0,2075	< LOD	0,1423	0,0045	0,0218	0,0123
Midden-Beemster	S311	V956	yes	No	YA	Female	1,3961	0,5449	< LOD	1,1322	6,5381	0,2468	0,113	17,0343	0,0144	0,2739	0,5643	0,0042	0,0597	0,0016	0,0342	0,0036
Midden-Beemster	S317	V0649	no	No	OA	Male	1,2366	0,6099	< LOD	0,6047	7,6064	0,3446	0,1036	19,3199	0,0092	0,1551	0,3976	< LOD	0,1859	0,0055	0,0258	0,0154
Midden-Beemster	S319	V0669	no	No	OA	Female	1,2752	0,5046	0,4323	2,2823	8,831	0,3138	0,1609	21,7431	0,0188	0,0139	0,135	< LOD	0,055	0,0072	0,0133	0,0115
Midden-Beemster	S370	V806	yes	Yes	MA	Female	1,4584	0,4204	< LOD	1,0713	7,0937	0,2712	0,1068	18,0046	0,0136	0,072	0,771	0,0119	0,1454	0,0084	0,0263	0,0231
Midden-Beemster	S374	V0861	no	No	OA	Male	1,6089	0,6021	< LOD	0,586	7,896	0,3123	0,1016	19,7907	0,0094	0,0251	0,273	0,0035	0,1162	0,0061	0,0147	0,0152
Midden-Beemster	S394	V869	yes	NA	OA	Female	1,343	0,5248	0,3163	2,1419	7,3161	0,3912	0,1762	19,0206	0,0252	0,0529	0,3075	0,0026	0,1372	0,0227	0,0208	0,0639
Midden-Beemster	S402	V0907	yes	No	MA	Male	2,0534	0,6336	0,7464	3,3112	8,3594	0,3055	0,1987	21,4343	0,0299	0,052	0,5824	0,0258	0,3464	0,0047	0,0242	0,0121
Midden-Beemster	S415	V9999	no	NA	OA	Male	1,4851	0,5613	< LOD	0,4046	7,1228	0,2957	0,0897	19,1134	0,0075	0,02	0,283	0,007	0,1856	0,0073	0,0123	0,0167
Midden-Beemster	S416	V1507	yes	Yes	MA	Male	1,3897	0,6311	1,0438	4,1979	7,2855	0,3242	0,308	20,7356	0,036	0,0651	0,7225	0,0013	0,088	0,0061	0,0181	0,0146
Midden-Beemster	S446	V944	yes	Yes	YA	Te checken	1,3362	0,5633	0,6406	3,2306	6,3952	0,3429	0,2149	18,7849	0,0301	0,1159	0,7438	0,0108	0,1948	0,0033	0,0248	0,0085
Midden-Beemster	S488	V1037	no	No	MA	Probable female	1,3362	0,5633	0,6406	3,2306	6,3952	0,3429	0,2149	18,7849	0,0301	0,1159	0,7438	0,0108	0,1948	0,0033	0,0248	0,0085
Midden-Beemster	S523	V1156	no	No	OA	Probable male	1,7736	0,5316	0,7074	2,4722	8,2316	0,3493	0,1791	21,8719	0,0189	0,04	0,3049	0,0106	0,0337	0,0056	0,0173	0,0199
Midden-Beemster	S524	V1120	no	No	MA	Male	1,1556	0,4405	0,3006	2,2942	7,515	0,2726	0,1752	18,6824	0,0219	0,1321	0,7918	0,0031	0,0942	0,0087	0,0242	0,0229
Midden-Beemster	S044	V0027	Yes	Yes	Child	NA	1,3283	0,5858	0,4959	3,2029	6,9788	0,2603	0,2265	18,5233	0,0272	0,0778	0,3739	0,0023	0,0869	0,0057	0,0283	0,0205
Midden-Beemster	S104	V0136	Yes	Yes	Child	NA	1,4357	0,514	0,7	3,6852	6,889	0,2736	0,25	18,4873	0,0328	0,1614	0,7043	0,0014	0,0615	0,0036	0,0249	0,0088
Midden-Beemster	S127	V0204	No	NA	Child	NA	1,6995	0,5172	< LOD	0,765	5,7789	0,2955	0,1046	16,1178	0,0079	0,0441	0,2246	0,0015	0,0992	0,0084	0,0269	0,0268
Midden-Beemster	S140	V0207	Yes	No	Child	NA	1,7991	0,6404	0,6439	3,6642	6,9609	0,2502	0,2253	18,3899	0,0326	0,0354	0,4066	0,01	0,1905	0,0067	0,0395	0,0177
Midden-Beemster	S141	V0223	Yes	NA	Child	NA	1,2478	0,6051	1,3714	6,3202	7,0425	0,3066	0,3766	19,8482	0,0673	0,0578	0,52	< LOD	0,0319	0,0081	0,0229	0,0257
Midden-Beemster	S167	V0267	Yes	No	Child	NA	1,8045	0,5708	0,1136	0,674	10,4228	0,4456	0,128	24,2284	0,0094	0,0043	0,1265	0,0015	0,0706	0,0035	0,0277	0,0128
Midden-Beemster	S181	V0407	Yes	NA	Child	NA	1,6832	0,5099	0,1742	1,4151	8,0875	0,3109	0,1448	20,669	0,0181	0,0502	0,7437	< LOD	0,0611	0,0049	0,0387	0,014
Midden-Beemster	S215	V0250	Yes	NA	Child	NA	1,3861	0,6399	0,4625	3,0026	7,0811	0,2533	0,1956	19,1338	0,0238	0,0188	0,2981	0,0024	0,0309	0,0047	0,0254	0,0151
Midden-Beemster	S248	V0393	Yes	NA	Child	NA	1,9163	0,6717	1,5028	5,5249	7,9332	0,3392	0,3217	22,4497	0,0425	0,0756	0,7226	0,0025	0,0793	0,0043	0,0322	0,011
Midden-Beemster	S282	V0417	Yes	Yes	Child	NA	1,8621	0,5974	< LOD	0,3734	9,9082	0,4484	0,1217	22,7999	0,0104	0,0073	0,1661	0,0018	0,0245	0,0034	0,0332	0,0119
Midden-Beemster	S286	V0469	Yes	No	Child	NA	1,4373	0,7151	1,3207	6,0297	6,8486	0,4085	0,4151	18,9208	0,0614	0,0952	0,669	0,0019	0,1156	0,0483	0,0226	0,1456
Midden-Beemster	S292	V0473	Yes	Yes	Child	NA	1,6187	0,515	0,3907	2,1659	8,6092	0,3062	0,161	20,9397	0,0258	0,1131	0,8054	0,0099	0,1213	0,0043	0,0255	0,0089
Midden-Beemster	S293	V0495	Yes	NA	Child	NA	1,4333	0,4707	0,3455	2,5434	6,3283	0,3647	0,1846	18,1229	0,0218	0,0147	0,3882	0,0443	0,1108	0,0089	0,0236	0,0146
Midden-Beemster	S301	V0583	Yes	NA	Child	NA	1,0365	0,5763	0,3576	2,2218	8,1492	0,254	0,1513	19,4695	0,0222	0,2904	0,6448	0,0112	0,136	0,0073	0,0264	0,0211
Midden-Beemster	S316	V0641	Yes	NA	Child	NA	1,3579	0,4608	0,18	1,2522	8,6532	0,3031	0,1277	21,7715	0,0133	0,043	0,4135	< LOD	0,0314	0,0038	0,0232	0,0077
Midden-Beemster	S326	V0708	Yes	Yes	Child	NA	1,6372	0,4193	0,0959	0,6051	8,497	0,3209	0,0969	20,2875	0,0047	0,0423	0,2396	0,0015	0,1002	0,0033	0,0253	0,0094
Midden-Beemster	S343	V0732	No	NA	Child	NA	1,1472	0,5847	1,3846	7,3227	3,5324	0,245	0,4488	13,7647	0,0728	0,0176	0,5961	0,002	0,0363	0,0052	0,0235	0,0141
Midden-Beemster	S353	V0739	Yes	Yes	Child	NA	1,445	0,6428	0,3947	2,7206	5,6582	0,2935	0,2032	16,6857	0,0297	0,0362	0,3136	< LOD	0,2812	0,0073	0,021	0,0231
Midden-Beemster	S367	V0803	Yes	No	Child	NA	1,0664	0,63	0,674	3,1963	7,6098	0,283	0,2381	19,626	0,0316	0,055	0,3559	0,0012	0,0647	0,0022	0,0223	0,008
Midden-Beemster	S396	V0877	Yes	No	Child	NA	1,5319	0,4099	0,1298	0,7564	9,2713	0,3226	0,1057	22,4251	0,0106	0,0535	0,3462	0,0015	0,0427	0,0034	0,0487	0,0097
Midden-Beemster	S412	V0888	Yes	No	Child	NA	1,3599	0,5384	0,1722	0,9953	8,7158	0,3172	0,1159	21,4375	0,0106	0,0546	0,356	0,0086	0,081	0,0079	0,0263	0,0177
Midden-Beemster	S443	V0922	No	Yes	Child	NA	1,5424	0,6524	1,4439	7,5643	5,7749	0,2764	0,4519	18,0152	0,0734	0,1828	1,2406	0,0036	0,0931	0,0044	0,0316	0,0111
Midden-Beemster	S463	V0988	No	No	Child	NA	1,2224	0,607	2,0817	9,3148	5,421	0,2182	0,5117	17,5866	0,0863	0,1019	0,987	0,0037	0,0387	0,0084	0,0251	0,0181
Midden-Beemster	S479	V1019	Yes	NA	Child	NA	1,3321	0,5302	1,4485	6,7576	7,2487	0,3224	0,3909	19,7756	0,0788	0,3099	0,7721	0,0024	0,0316	0,002	0,0243	0,0042
Midden-Beemster	S503	V1099	Yes	No	Child	NA	1,476	0,5917	< LOD	0,1687	9,5738	0,3123	0,0803	23,0388	0,0086	0,2538	0,4437	0,0313	0,1758	0,0134	0,0335	0,0194
Midden-Beemster	S515	V1111	Yes	NA	Child	NA	1,1827	0,593	1,1518	5,0956	7,0263	0,2862	0,2771	21,0233	0,0379	0,0408	0,4849	< LOD	0,0907	0,0027	0,024	0,0125
Midden-Beemster	S549	V1181	Yes	No	Child	NA	1,9622	0,5632	0,7132	3,3615	7,7539	0,3398	0,1928	20,1945	0,0341	0,0546	2,3133	0,0022	0,0515	0,0068	0,0466	0,0119
Midden-Beemster	S123	V182	Yes	NA	Adolescent	NA	1,4918	0,5778	0,7405	4,5139	7,0029	0,2562	0,3264	18,0221	0,0585	0,4365	1,1024	0,0029	0,16	0,0053	0,0304	0,0133

Midden-Beemster	S206	V353	Yes	NA	Adolescent	NA	1,571	0,5328	0,0772	1,0018	8,5135	0,3057	0,1102	21,6668	0,0142	0,5005	0,6714	0,002	0,063	0,0029	0,0346	0,0073
Midden-Beemster	S229	V324	No	No	Adolescent	NA	1,1683	0,5164	1,3641	5,3173	6,8072	0,3455	0,388	21,0916	0,0467	0,303	0,7081	< LOD	0,045	0,0023	0,0187	0,0089
Midden-Beemster	S246	V396	No	Yes	Adolescent	NA	1,9456	0,5227	0,1551	1,0614	9,318	0,3005	0,121	23,4114	0,0111	0,1792	0,164	< LOD	0,0434	0,0026	0,0204	0,007
Midden-Beemster	S275	V526	Yes	No	Adolescent	NA	1,7621	0,4261	0,1772	1,0124	9,7554	0,386	0,1482	23,4085	0,0148	0,0476	0,373	< LOD	0,0275	0,0032	0,0259	0,0102
Midden-Beemster	S307	V591	Yes	No	Adolescent	NA	1,698	0,4733	< LOD	1,0442	7,0114	0,2587	0,1221	18,6193	0,0132	0,0173	0,2393	< LOD	0,042	0,0031	0,02	0,0092
Midden-Beemster	S462	V987	Yes	Yes	Adolescent	NA	1,7495	0,5654	0,9612	4,69	6,4428	0,2643	0,3436	17,298	0,0561	0,1237	0,924	0,0013	0,0649	0,0072	0,0234	0,0163
Midden-Beemster	S454	V963	Yes	No	Adolescent	NA	1,7965	0,3784	0,4162	1,6687	8,8281	0,3622	0,1295	22,3974	0,0235	0,0963	1,736	0,0016	0,0396	0,01	0,0316	0,021
Midden-Beemster	S479	V1014	Yes	NA	Adolescent	NA	1,3674	0,6928	1,548	7,5575	6,0999	0,3016	0,4819	17,7606	0,0934	0,2865	0,9256	0,0026	0,0297	0,0019	0,0231	0,0038
Midden-Beemster	S507	V1093	Yes	UNOB	Adolescent	NA	2,2945	0,549	0,4493	1,742	10,7227	0,311	0,1505	24,7212	0,0233	0,1628	0,4823	0,0015	0,0621	0,0038	0,0455	0,0086
Arnhem	S280	V218	No	No	MA	Female	1,7483	0,4854	< LOD	0,5434	7,271	0,2705	0,1056	17,81	0,019	0,1525	0,9206	0,0029	0,0739	0,0044	0,0147	0,0115
Arnhem	S258	V246	No	No	MA	Male	1,7475	0,4611	0,3327	1,2233	8,4858	0,2046	0,1989	19,5318	0,0384	0,2551	1,1262	0,0046	0,0688	0,0028	0,0181	0,0062
Arnhem	S371	V481	No	UNOB	MA	Male	1,8929	0,4354	0,2023	1,0134	10,5694	0,1971	0,1062	23,5556	0,0111	0,0343	0,1178	< LOD	0,1073	0,0014	0,0166	0,0038
Arnhem	S370	V492	No	No	MA	Probable Male	1,5647	0,6033	0,7104	2,2473	10,426	0,2048	0,1948	23,2918	0,0376	0,0368	0,4118	0,005	0,1474	0,0018	0,0241	0,0058
Arnhem	S438	V687	No	No	YA	Probable Female	1,3327	0,7048	0,6658	2,2112	9,6715	0,1924	0,1856	22,7037	0,0284	0,0124	0,1772	0,0031	0,0631	0,0009	0,0241	0,0023
Arnhem	S520	V0814	No	No	OA	Female	1,3211	0,4831	0,0944	0,6478	8,885	0,1945	0,1091	20,0109	0,0133	0,0115	0,117	0,0014	0,0584	0,0027	0,0157	0,0084
Arnhem	S529	V863	No	No	OA	Male	1,4199	0,4354	0,5923	1,2681	10,3934	0,2022	0,1757	23,4874	0,0252	0,0115	0,2583	0,0052	0,053	0,003	0,019	0,009
Arnhem	S537	V868	No	Yes	MA	Male	1,5793	0,5299	0,4805	1,0582	10,6152	0,2042	0,1403	23,8549	0,0207	0,0306	0,2695	0,0062	0,1725	0,0018	0,0296	0,0039
Arnhem	S539	V0855	No	No	YA	Probable Female	1,8534	0,5493	0,1774	0,4274	9,7982	0,2173	0,1	22,4318	0,0135	0,0204	0,2087	0,0029	0,2069	0,0026	0,0182	0,0075
Arnhem	S597	V1043	No	No	OA	Male	1,5661	0,559	< LOD	0,6862	9,8213	0,2861	0,1127	21,8131	0,0096	0,0154	0,1575	0,001	0,0917	0,0061	0,0143	0,0218
Arnhem	S604	V1087	No	No	MA	Probable Female	1,3614	0,5836	0,1838	0,8173	9,2088	0,1804	0,1188	21,07	0,016	0,0089	0,1356	0,0036	0,1254	0,0015	0,0228	0,0041
Arnhem	S639	V1247	No	No	YA	Probable Female	1,4913	0,5455	0,3852	1,199	8,4236	0,1488	0,1388	18,8385	0,0301	0,0769	0,4177	0,007	0,1319	0,002	0,0245	0,0065
Arnhem	S648	V1298	No	UNOB	MA	Probable Male	1,6892	0,4981	0,1131	0,6803	9,118	0,2022	0,1008	20,6829	0,0132	0,0248	0,1484	0,0045	0,0987	0,0019	0,0187	0,0046
Arnhem	S659	V1298	No	No	OA	Male	1,5969	0,4636	0,1198	0,6577	9,4805	0,2054	0,1234	21,4136	0,0141	0,0063	0,1098	0,0019	0,0631	0,0008	0,0179	0,0022
Arnhem	S660	V1299	No	No	MA	Male	1,5436	0,5744	0,2286	0,969	9,3545	0,2411	0,1213	21,7917	0,0122	0,0325	0,1907	0,0014	0,0502	0,0031	0,0129	0,0093
Arnhem	S683	V1346	No	No	YA	Probable Male	1,6918	0,4458	< LOD	< LOD	9,8781	0,1883	0,0836	21,3251	0,0121	0,1049	0,8698	0,0061	0,1291	0,0024	0,0229	0,0061
Arnhem	S719	V1428	No	UNOB	MA	Probable Male	1,7087	0,4581	0,294	0,6514	10,3024	0,2332	0,123	22,7576	0,0103	0,0068	0,157	0,0034	0,0846	0,0015	0,0142	0,0041
Arnhem	S0722	V1434	No	No	YA	Female	1,4431	0,4241	< LOD	0,0814	9,7238	0,1924	0,0844	21,7834	0,0082	0,0164	0,1629	0,0023	0,0847	0,001	0,0143	< LOD
Arnhem	S0723	V1436	Yes	No	MA	Female	1,7121	0,3725	0,1062	0,325	10,1785	0,2282	0,0944	22,9974	0,0112	0,0238	0,149	< LOD	0,0743	0,0027	0,0128	0,0105
Arnhem	S750	V1495	No	No	YA	Probable Male	1,5111	0,6534	0,9919	3,3445	9,404	0,1959	0,2406	22,9707	0,044	0,0354	0,378	0,004	0,0951	0,0022	0,0218	0,0068
Arnhem	S853	V1727	Yes	No	YA	Probable Female	1,1171	0,3659	0,4243	1,1552	8,4291	0,1786	0,1309	20,4265	0,0206	0,1855	0,2823	0,0072	0,1351	0,0044	0,0121	0,0139
Arnhem	S918	V1881	No	No	YA	Probable Male	1,8159	0,4874	0,1032	0,7531	8,6722	0,2205	0,1111	20,9577	0,0113	0,1233	0,3772	0,0028	0,0712	0,0032	0,0141	0,0107
Arnhem	S961	V1967	No	No	OA	Probable Male	2,1811	0,4927	0,1734	0,3226	8,693	0,1902	0,0962	21,5301	0,0144	0,1989	0,2719	0,006	0,0651	0,0024	0,0142	0,0074
Arnhem	S1270	V2484	Yes	Yes	YA	Female	1,5676	0,4768	0,0862	0,5203	8,9707	0,1876	0,1011	21,3597	0,0147	0,011	0,1989	0,0049	0,291	0,0017	0,0218	0,0036
Arnhem	S1096	V2168	No	No	MA	Probable Male	1,4847	0,5449	0,3414	1,0778	7,8045	0,1993	0,1259	19,0144	0,0247	0,354	0,7694	0,0085	0,1257	0,0039	0,0229	0,0089
Arnhem	S375	V420	Yes	Yes	Adolescent	NA	1,2056	0,434	0,2549	1,8078	7,3865	0,2273	0,1801	17,9509	0,0269	0,0265	0,3327	0,0043	0,2088	0,0036	0,0156	0,011
Arnhem	S407	V533	Yes	UNOB	Adolescent	NA	1,9886	0,4165	0,2717	0,7139	9,3134	0,2081	0,1124	22,0954	0,0244	0,0616	0,3646	0,0069	0,1745	0,0025	0,0243	0,0066
Arnhem	S409	V528	Yes	No	Adolescent	NA	1,3368	0,5765	0,9081	2,6406	9,9342	0,1914	0,2168	22,5562	0,0363	0,0438	0,3258	0,0081	0,0824	0,003	0,0235	0,0062
Arnhem	S863	V1753	Yes	Yes	Adolescent	NA	1,2837	0,5268	0,1657	0,9956	8,0161	0,1885	0,1374	18,8618	0,0247	0,4033	0,5913	0,0055	0,1012	0,0009	0,0201	0,0033
Arnhem	S1193	V2357	Yes	Yes	Child	NA	2,3083	0,4741	0,2785	0,6426	9,8075	0,1928	0,1176	21,2385	0,0261	0,9192	0,846	0,0112	0,1372	0,0052	0,0255	0,0138
Arnhem	S404	V548	Yes	No	Child	NA	1,268	0,4921	0,1627	0,3126	10,4469	0,172	0,087	21,3815	0,0183	0,0549	0,4015	0,0064	0,0796	0,0018	0,0145	0,004
Arnhem	S1051	V2110	Yes	UNOB	Child	NA	1,0998	0,5806	1,1645	4,0462	6,0466	0,1389	0,3031	16,695	0,0484	0,2224	0,4043	0,0074	0,0827	0,0034	0,0198	0,0105
Arnhem	S936	V1912	Yes	Yes	Adolescent	NA	1,8366	0,4431	0,1293	0,2976	11,2605	0,1918	0,0973	24,1051	0,0137	0,0528	0,158	0,0068	0,1282	0,0009	0,0255	0,0035
Arnhem	S411	V556	No	UNOB	Adolescent	NA	1,8622	0,5746	0,489	1,6884	8,4717	0,2041	0,1578	19,3726	0,035	0,4478	0,981	0,0089	0,2816	0,0082	0,0237	0,018
Arnhem	S889	V1813	Yes	Yes	Adolescent	NA	1,3977	0,3074	< LOD	0,1227	10,3791	0,236	0,087	23,0421	0,0074	0,0222	0,1482	0,0015	0,1181	0,0013	0,0149	0,0048
Arnhem	S731	V1457	Yes	Yes	Adolescent	NA	1,7329	0,623	0,1523	0,352	10,621	0,1917	0,1071	22,976	0,014	0,0134	0,1982	0,0057	0,1733	0,001	0,0203	0,0038
Arnhem	S447	V685	Yes	Yes	Adolescent	NA	1,9095	0,5823	0,1234	< LOD	10,8111	0,1873	0,0855	23,3446	0,014	0,0124	0,2924	0,0054	0,1936	0,0024	0,026	0,0041
Arnhem	S758	V1521	No	Yes	Adolescent	NA	1,7417	0,5451	0,0921	0,2144	9,6826	0,1753	0,0879	20,9278	0,0207	0,1378	0,5324	0,0042	0,0916	0,0012	0,0235	0,002